QUANTUM MAGNETIC COLLAPSE IN NEUTRON STAR BINARY SYSTEMS

by

Craig Lee Brooks, B.A.

THESIS

Presented to the Faculty of

University of Houston-Clear Lake

In Partial Fulfillment

Of the Requirements

For the Degree

MASTER OF SCIENCE

in Physics

THE UNIVERSITY OF HOUSTON-CLEAR LAKE

May, 2019

QUANTUM MAGNETIC COLLAPSE IN NEUTRON STAR BINARY SYSTEMS

by

Craig Lee Brooks

APPROVED BY:

Samina Masood, PhD, Chair

David Garrison, PhD, Committee Member

Van Eric Mayes, PhD, Committee Member

APPROVED BY THE COLLEGE OF SCIENCE AND ENGINEERING:

Said Bettayeb, PhD, Associate Dean

Ju H. Kim, PhD, Dean

Dedication:

To my Mother, for cheering me on through this journey, and my Father, who encouraged me at a young age to pursue science, to my family, and to the ancestors.

Acknowledgments:

I would like to thank Dr. Samina Masood, who made sure I didn't go off course in completing my thesis, my committee Dr. David Garrison and Dr. Van Eric Mayes, and the staff and advisors of AstroComNYC for exposing me to astrophysics research, and to the many friends I've made along the way.

ABSTRACT

QUANTUM MAGNETIC COLLAPSE IN NEUTRON STAR BINARY SYSTEMS

Craig Lee Brooks

University of Houston-Clear Lake, 2019

Thesis Chair: Samina Masood, PhD

Quantum magnetic collapse is a phenomenon that corresponds to the collapsing of stars due to the generation of high magnetic field. Such stars are highly magnetized objects (such as neutron stars) where the particle processes take place in the presence of very high external magnetic field B. When the magnetic energy inside the star exceeds the internal energy of electrons and/or positrons fluids it will lead to breaking of hydrostatic equilibrium. In the astrophysical context, this will occur when B corresponding to electron mass (10^{13} Gauss). At this energy, there is a collapse of the neutral matter with a magnetic moment since the pressure transverse to the magnetic field vanishes. Typically, we would calculate the magnetization and particle number N of this system using derivatives of the thermodynamic potential Ω with respect to magnetic field and chemical potential, but this can be difficult since Ω diverges. Additionally, for neutron stars, we would like to consider how

these quantities may change as electrons are accreted onto the neutron star. We develop a method for calculating the particle number N in the static case, then extend this to the accreting system to calculate the dynamical particle number density with the orientation of using this result for calculating the magnetization as it changes in time.

TABLE OF CONTENTS

LIST OF TABLES

LIST OF FIGURES

CHAPTER I:

INTRODUCTION

This thesis will proceed as follows: Chapter II will analyze accretion processes and study the two main models, which are thin disc accretion and Bondi-Hoyle accretion. We will look at the mechanics, energetics, and thermodynamic properties of each model.

Chapter III proceeds by discussing the properties of neutron stars and how they are formed. The ideal gas equation of state will be derived that forms the basis of the original neutron star models proposed by Baade and Zwicky [2] and later detailed by Oppenheimer and Volkoff [28]. Next, we discuss the types of neutron stars such as magnetars and pulsars, then compare the different binary configurations in which they exist,

Chapter IV discusses the phenomena of quantum magnetic collapse in detail, explaining the conditions leading up to collapse with a focus on the particle number density, ground state energy, and anisotropic pressures from the induced magnetization of the constituent particles. A quantum statistical mechanics approach is used to develop a calculation scheme is developed to determine the particle number density with the orientation to calculate the magnetization as a function of the number density.

In the final Chapter V, a scheme for variable number density will be developed with the results from Chapter 4 as a basis. This scheme will examine how the particle number density changes in time during the accretion process in binary systems. We then determine the limitations on the accretion

process in the limit that radiation pressure is greater than the gravitational force, and when the gravitational force is greater than the radiation pressure and set a temperature scale for when the accretion process is steady (hydrodynamics equilibrium). In the discussion we will present a summary of these results.

CHAPTER II:

ACCRETION

In astrophysics, a binary system are two bodies that orbit each other around their mutual center of gravity. Most often, we are considering two stars or a black hole and a star. We call the accreting object the *primary* and the donating star the *secondary*.

If the primary is sufficiently massive, and the secondary is sufficiently close, the primary may begin to accrete matter from the secondary onto itself. Since this process is essentially a transfer of matter and energy, it is more appropriate to study the details of this process, and then discuss observations of X-ray binaries and how strongly they align with theoretical models.

Thin disc Accretion: Mechanics

In strong magnetic fields, the accretion tends to be channeled to the poles and is nonsteady. This occurs when the magnetic field is of the order of $B < 10^8 G$. [43] At these field strengths, some portion of the matter will follow the magnetic field lines from the equatorial latitude to the poles.[21][29]

We will begin by making a few assumptions to simplify our analysis. First, assume that the fluid is electrically neutral. This would also entail that $n_+ = n_-$ where n_+ is the number density of positive charges and n_- the number density of negative charges.

We will consider a simplified binary accretion where the particles initially

assume a Keplerian orbit around the neutron star. At this point it will serve us well to understand the limits of a stable fluid flow from the secondary.

For a Keplerian orbit of particles of mass m and radius r from the neutron star, the total energy can be written as

$$E = \frac{1}{2}mv^2 + \frac{D}{r} \tag{2.1}$$

Where $\frac{D}{r} = \frac{GMm}{r} + \frac{kQq_lR^2}{r^3}$. Here, the second term in $\frac{D}{r}$ gives us the electromagnetic contribution to the effective potential, where k $= \frac{1}{4\pi\epsilon_0}$, q is the charge of particle species l, and Q is the bulk charge in the region of the neutron star.

We will proceed by using the treatment used by Melia [21]. For a thin disc accreting onto a star, the geometry is axially symmetric, so it is suitable to carry out the analysis in cylindrical coordinates. Let us consider gas elements in the disc α' and β at different locations which move radially outward and inward, respectively. Element α has an azimuthal velocity v_{ϕ_α} denoted as

$$v_{\phi_\alpha} = R\Omega(R) \tag{2.2}$$

where R is the radial position of the mass element at α and $\Omega(R)$ is the angular velocity at point R.

The specific angular momentum contribution $\delta l'_{\alpha\to\alpha}$ from point α to α' is

$$\delta l_{\alpha\to\alpha'} = (R+\lambda)R\Omega(R) \tag{2.3}$$

where λ is the scale length, which is the distance over which particular quantity decreases by a factor of e. In this case, the specific quantity decreas-

ing ove this scale length is the angular momentum. β, on the other hand, takes azimuthal velocity

$$v_{\phi_{\beta' \to \beta}} = (R + \lambda)\Omega(R + \lambda) \tag{2.4}$$

and contrinbutes to the specific angular momentum

$$\delta l_{\phi_{\beta' \to \beta}} = R(R + \lambda)\Omega(R + \lambda) \tag{2.5}$$

Since these two elements have different angular momenta, a torque τ_{out} is exerted by the inner element on the outer element

$$\tau_{out} \approx \dot{M}_{\alpha \to \alpha'}(R + \lambda)R\Omega(R) - \dot{M}_{\beta' \to \beta}R(R + \lambda)\Omega(R + \lambda) \tag{2.6}$$

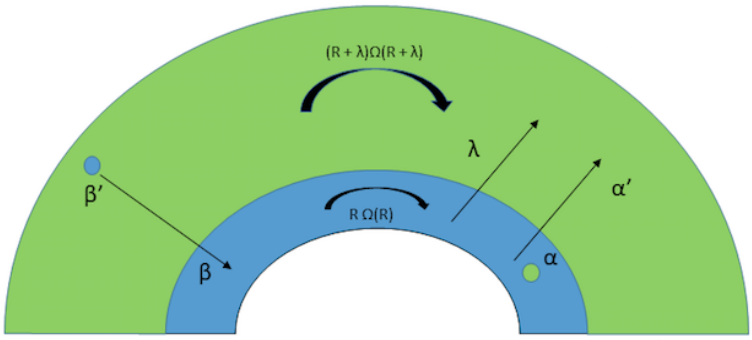

Figure 2.1: Neighboring disc rings exchange matter, the outer ring from B' and the inner from A. As the azimuthal velocities are not the same, they carry angular momentum away from their respective locations, resulting in a net torque on the outer ring.

where $\dot{M}_{\alpha \to \alpha'}$ is the mass-loss rate from radial location α to α' in the accretion disc. For a *steady state* disc of thickness H

$$\dot{M}_{\alpha \to \alpha'} = \dot{M}_{\beta' \to \beta} = (2\pi RH)\rho(R)v_R \tag{2.7}$$

where v_R is the velocity, ρ is the density of the disc at radius R.

Let us define the *surface density* $\Sigma \equiv \rho H$ and the *shear viscosity* $\nu \equiv \lambda v_R$. By these definitions, the torque is then defined as

$$\tau_{out} = -2\pi\nu\Sigma R^3\Omega \tag{2.8}$$

Since $\Omega(R)$ decreases as the radius R from the central accretor increases, then $\tau > 0$, so the outer elements will spiral in slower than the inner elements.

Close to the orbital plane

$$v_\phi(R) = R\Omega_k(R) \tag{2.9}$$

where

$$\Omega(R)_k \equiv \left(\frac{GM}{R^3}\right)^{1/2} \tag{2.10}$$

is defined as the Keplerian angular velocity. If R is a radial location on the disc and ΔR is the differential change in the radius, then between R and ΔR, the mass M and angular momentum L are

$$M = 2\pi R\Delta R\Sigma \tag{2.11}$$

$$L = (2\pi R\Delta R\Sigma)R^2\Omega \tag{2.12}$$

We can calculate the mass loss rate $\dot{M}_i$ by letting $R' = R + \Delta R$ equal the new radial position by

$$\frac{dM_i}{dt} = \frac{d}{dt}(2\pi R\Delta R\Sigma) = v_R 2\pi R\Sigma_R - v_{R'} 2\pi R'\Sigma_{R'} \tag{2.13}$$

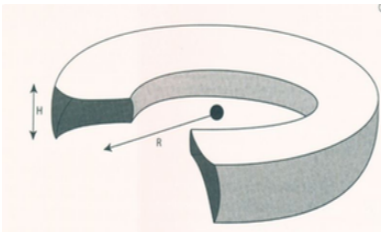

Figure 2.2: While motion of matter in the Z - axis is suppresssed by collisions, particles will move azimuthally so that angular momentum is conserved Source:[21]

$$\frac{dM_i}{dt} \approx -2\pi\Delta R\frac{d}{dR}(R\Sigma v_R) \tag{2.14}$$

where v_R is the radial velocity inward at $R(orR')$ and Σ_R (or Σ'_R) is the surface density at $R(orR')$

$$\rightarrow R\frac{d\Sigma}{dt} + \frac{d}{dR}(R\Sigma v_R) = 0 \ (conservation\ of\ mass\ for\ disc) \tag{2.15}$$

Where v_R is the velocity at R. Because we assumed Keplerian orbits of the accreting material from the outset,$\Omega \rightarrow \Omega_k$, thus

$$\frac{1}{2}R\Sigma v_R\left(\frac{GM}{R}\right)^{1/2} = \frac{d}{dR}\left[\frac{-3}{2}(GMR)^{1/2}\nu\Sigma\right] \tag{2.16}$$

Therefore, the radial velocity v_R is

$$v_R = -\frac{3}{\Sigma R^{1/2}}\frac{d}{dR}(\nu\Sigma R^{1/2}) \tag{2.17}$$

If ν is constant (steady state) then $R\Sigma v_R$ is also constant and the accretion rate is

$$\frac{dM}{dt} = 2\pi R\Sigma(-v_R) \tag{2.18}$$

Power and Energy of Accretion

Since some portion of the gravitational potential energy is converted into kinetic and thermal energy, necessarily this fraction of gravitational energy is radiated away, and the rest is advected inward [21]. Keeping with thin-disc accretion theory, the assumption is that all the energy is radiated from the same location. The corresponding change in the torque on a ring of material can be calculated by,

$$\tau_{out}(R) - \tau_{out}(R + \Delta R) = -\frac{d\tau_{out}(R)}{dR} dR \tag{2.19}$$

We now want to caculate the power exerted on the ring through viscosity

$$P = -\Omega \frac{d\tau_{out}(R)}{dR} dR = -\frac{d}{dR} \left[\tau_{out}\Omega - \tau_{out}\Omega'\right] \tag{2.20}$$

$$P = \int_{R_{in}}^{R_{out}} \frac{d}{dR} \left(\tau_{out}\Omega\right) dR = \tau_{out}\Omega|_{out} - \tau_{out}\Omega|_{in} \tag{2.21}$$

this means the contributions to the total power are determined by the inner and outer edges of the disc. [21]. In the power equation (2.20), the second term gives the local heat dissipation. Given that the total surface area per ring is $2(2\pi R)dR$, where dR is the width of the ring, then the dissipation rate per unit surface area $D(R)$ is

$$D(R) = \frac{\tau_{out}\Omega'}{4\pi R} = -\frac{1}{2}\nu\Sigma(R\Omega')^2 \tag{2.22}$$

Unfortunately, it is not always feasible to determine the viscosity ν from first principles. Instead we have observables which will allow us to obtain the dispersion.

From Melia [21], we can let the angular momentum equation to be

$$R\frac{d}{dt}(\Sigma R^2\Omega') + \frac{d}{dR}(R\Sigma v_R R^2\Omega) = -\frac{1}{2\pi}\frac{d}{dR}\tau_{out} \tag{2.23}$$

If we use Equations 2.23 and 2.15, maintaining the steady state, which means angular momentum is conserved, by setting the change in angular momentum to zero, we obtain

$$R\Sigma v_R R^2\Omega = -\frac{1}{2}\tau_{out} + C \tag{2.24}$$

Substituting 2.8 for τ_{out}, we obtain

$$\nu\Sigma\Omega' = \Sigma(v_R)\Omega + \frac{C}{R^3} \tag{2.25}$$

where C is a constant. The rotational velocity of the disc near a neutron star must match the rotation of the neutron star in order for accretion to occur. Letting $\Omega' \to 0$ and $\Omega = \Omega_k(R_*)$ where R_* is the radius of the neutron star, this leads to

$$\frac{\dot{M}}{2\pi}(GMR_*)^{1/2} = C \tag{2.26}$$

Therefore,

$$D(R) = \frac{3GM\dot{M}}{8\pi R^3}\left[1 - \left(\frac{R}{R_*}\right)^{1/2}\right] \tag{2.27}$$

Thus, we have an expression for the dissipation rate of the heat per unit volume in terms of observables. In the next section, we will examine an accretion process where, instead of the disc structure we are accustomed to, the matter accretes radially onto the primary.

Bondi-Hoyle Accretion

We are able to detect compact objects usually because they accrete material from the surrounding environment. Most notably, active galactic nuclei (AGN's), the supermassive black holes that are in the center of galaxies, are the most obvious case for this kind of observation.

However, in tight binary systems, the companion member may exceed its *tidal radius*, the distance which a celestial object from another celestial object when, if exceeded, will cause the object to lose hydrostatic equilibrium and be ripped apart. This tends to happen the companion object expands during its evolution. This is the scenario of accretion for high mass X-ray binaries (HMXBs), which will be discussed in the next chapter,

In the following sections we will examine how we determine the tidal radius, the mechanics of Bondi-Hoyle accretion and its relationship to thermodynamic properties, and more realistic accretion models.

Determining the Tidal Radius: The Roche Limit

The tidal radius can be determined by considering the effective mass u at the point of interaction that exists on the surface of a satellite on the side closest to the primary, and assume the satellite is in freefall (i.e. no other forces other than the tidal forces are relevant). We can then find the differential force from the primary to the edge of the satellite and the center of mass

The gravitational force F_{g_u} on mass u from the satellite of mass m and radius r is

$$F_{g_u} = \frac{Gmu}{r^2} \tag{2.28}$$

The tidal force is found exactly by taking the difference between the primary's attraction on the center of mass of the secondary and that of the mass element u on the surface.

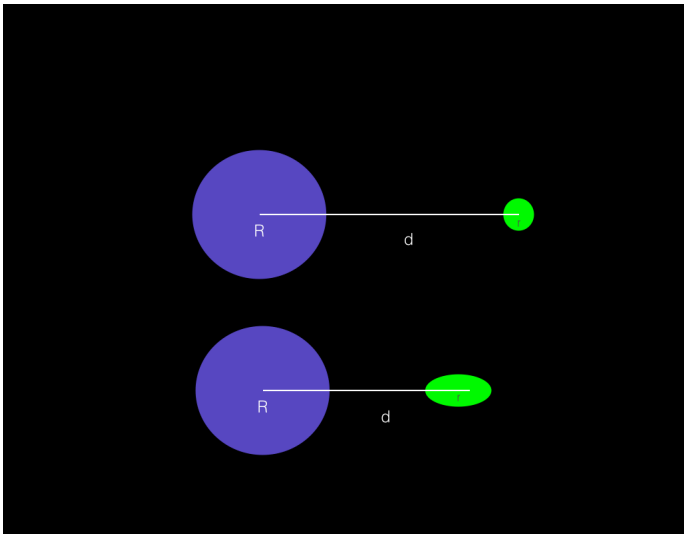

Figure 2.3: Depiction of the Roche limit with 2 massive bodies with centers of masses at distance d and radii R and r. On top, the body is outside the Roche limit, on bottom, the smaller body has exceed the tidal radius

$$F_T = \frac{GMu}{(d-a)^2} - \frac{GMu}{d^2} \tag{2.29}$$

Factoring out GMu and finding a common denominator $d^2(d-a)^2$

$$F_T = (GMu)\frac{d^2 - (d-a)^2}{d^2(d-a)^2} \tag{2.30}$$

$$F_T = (GMu)\frac{d^2 - (d^2 - 2ad + a^2)}{d^2(d^2 - 2ad + a^2)} \tag{2.31}$$

$$F_T = (GMu)\frac{d^2 - d^2 + 2ad - a^2}{d^4 - 2ad^3 + (ad)^2} \tag{2.32}$$

where r is the radius of the satellite and d is the separation distances

between the centers of mass of the primary and satellite. Let $a << R$ and $R < d$ with R being the radius of the primary. Under these conditions, all the terms in with a^2 in the numerator and denominator and a in the denominator are ignorable. The tidal force F_T on mass u toward the primary of mass M can then be expressed as

$$F_T = GMu\frac{2dr}{d^4} = \frac{2GMur}{d^3} \tag{2.33}$$

When the tidal force on mass element u is balanced by the gravitational force from the satellite, the Roche limit, or tidal radius, is reached.

$$F_{g_u} = F_T \tag{2.34}$$

Therefore

$$\frac{2GMua}{d^3} = \frac{Gmu}{a^2} \rightarrow 2a^3\frac{M}{m} = d^3 \rightarrow d = a\left(\frac{2M}{m}\right)^{\frac{1}{3}} \tag{2.35}$$

If $M \sim 10^6$, we can drop the factor of 2, for an order of magnitude calculation.

Bondi Accretion

Accretion can occur in several astrophysical forms, such as accretion onto a black hole, infalling of matter into a galactic cluster, or perhaps infalling of matter into a star. To simplify our understanding of this process, we assume a spherically symmetric system, like a star. We can also assume that the flow is smooth and the viscosity is insignificant. Stellar winds and/or shocks may be associated with accretion events. Because the solutions to

the fluid equations must satisfy very different conditions at the same point, these solutions are discontinuous.

Although it is not common that matter would fall radially towards the source of gravity, spherical accretion can be useful when analyzing matter accreting in deep potential wells [21]. This can happen when the donor object is relatively far away from the accreting object (as in the case of high mass X-ray binaries)

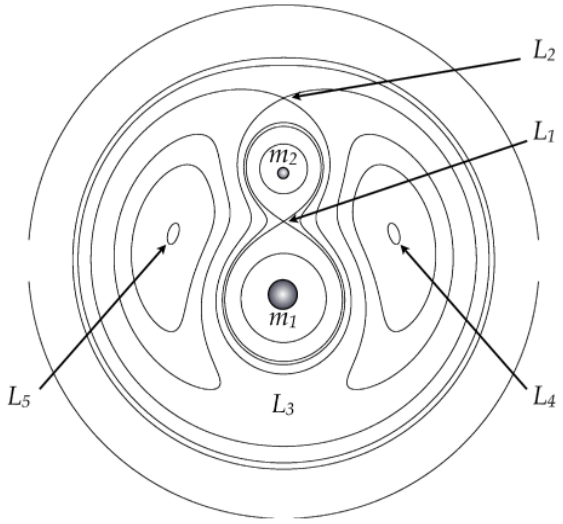

Figure 2.4: Top view of the orbital plane displaying Roche equipotential lines. A test particle places on any particular line will continue on the same trajectory. Source: [5]

At this point, we would like to examine how material falls onto some central mass from the radial direction in some environments. This theory of accretion is called $Bondi - Hoyle\ accretion$. We would like to use this theory primarily because it allows us to examine accreting systems in terms of thermodynamic quantities, which will be much simpler than the treatment in the previous section. In the following sections, we will develop an expression

for the accretion rate by using the enthalpy into the momentum equation for fluids.

Fluid Mechanics of Bondi-Hoyle Accretion

As a simplifying assumption, let us take the pressure p of the fluid to be a function of its density only, and is a $barotropic function$. The enthalpy h is defined as

$$h = \int \frac{dp}{\rho} \tag{2.36}$$

Where ρ is the density of the fluid [42]. Taking the gradient, we obtain

$$\nabla h = \frac{\nabla p}{\rho} \tag{2.37}$$

We can then write the *momentum equation* for a nonviscous fluid using the convective derivative as

$$\rho \frac{D\mathbf{v}}{Dt} = -\nabla p - \rho \nabla \psi \tag{2.38}$$

Where v is some macroscopic property of the fluid (in this case velocity) and ψ is the potential function. The *convective derivative*, $\frac{D}{Dt}$, describes how the velocity of a matter element changes as a function of position and time. From this, we can obtain the continuity equation as well.

Using the vector calculus identity,

$$\frac{1}{2}(\mathbf{v} \cdot \mathbf{v}) = (\mathbf{v} \cdot \nabla)\mathbf{v} + \mathbf{v} \times (\nabla \times \mathbf{v}) \tag{2.39}$$

and knowing that $(\mathbf{v} \cdot \nabla)\mathbf{v} = 0$ since the change in the velocity is perpendicular to the flow of the fluid. By rearranging, we can show that

$$\nabla\frac{1}{2}v^2 - \mathbf{v}\times(\nabla\times\mathbf{v}) = -\frac{1}{\rho}\nabla p - \nabla\psi \tag{2.40}$$

And inserting the gradient of the enthalpy, we obtain

$$\mathbf{v}\times(\nabla\times\mathbf{v}) = \nabla(\frac{1}{2}v^2 + h + \psi) \tag{2.41}$$

$$\rightarrow \mathbf{v}\cdot\nabla(\frac{1}{2}v^2 + h + \psi) = 0 \tag{2.42}$$

As is shown, the quantity $v^2/2 + h + \psi$ is constant along all streamlines of the fluid. This result is called *Bernoulli's theorem*, which states that the pressure or the potential energy in a flowing fluid must decrease if the velocity of the fluid increases. Stated another way, it says that the energy of the accretion flow must be conserved.

We can now use this result to proceed in our discussion of Bondi accretion, and therefore determine the radius at which matter begins to accrete from a binary companion. Let us consider a system such as a neutron star that is accreting from a stellar companion that is accreting smoothly with a pressure $p = P(\rho)$ and ignore effects from the self gravity of the accreting gas and assume a viscosity that is negligible. Integrating the continuity equation, we obtain

$$4\pi r^2\rho v = -\dot{M} = constant \tag{2.43}$$

The above is known as the *Bondi accretion rate.* If the flow is isothermal, $p = \rho {v^2}_{sound}$, where ${v^2}_{sound}$ is the speed of sound in the medium.

Going back to the Bernoulli equation, we can set v = 0 and then

$$h - GM/r = \frac{p}{\rho} \rightarrow {v^2}_{sound} = \frac{GM}{r_B} \tag{2.44}$$

$$r_B = \frac{GM}{{v^2}_{sound}} \tag{2.45}$$

This yields the *Bondi radius*, which is the distance at which matter begins to accrete from the secondary to the primary. From this derivation, it can be shown that from a few thermodynamic quantities such as the enthalpy, pressure, and potential energy, we can determine required thermodynamic parameters to have a better understanding of hydrodynamic equilibrium.

Additional Thermodynamic Quantities

Clearly, an accreting fluid will have a force, energy, and other thermodynamic quantities associated with it. Obtaining these quantities is relatively straightforward. Starting from the first law of thermodynamics

$$du = Tds + Pdv \tag{2.46}$$

Keeping the same assumption that the density of the fluid is constant, which means that $\frac{P}{\rho^2}\frac{d\rho}{dt} = 0$. Thus, we obtain the entropy from simply rearranging the above equation and integrating.

$$\frac{du}{dt} = T\frac{ds}{dt} + \frac{P}{\rho^2}\frac{d\rho}{dt} \tag{2.47}$$

$$\rightarrow du\frac{dt}{dt} = Tds \tag{2.48}$$

$$\rightarrow \int \frac{du}{T} = \int ds \tag{2.49}$$

In summary, the enthalpy and pressure are two thermodynamic quantities that govern the fluid flow in accreting systems. From this fluid flow, we can easily understand when matter will begin to accrete by calculating the Bondi radius. Thermodynamic potentials are directly calculable from the first law, and we can therefore understand other properties of the accretion process as it evolves in time. In addition, we can show that the energy and mass is conserved in the accretion flow given certain assumptions in the analysis.

Realistic Accretion Model

At this point, we will discuss the properties of X-Ray binary accretion using the model proposed by Pringle and Rees[32] . The model for the accretion disc typically depends on the assumptions about the macroscopic properties such as viscosity or turbulence. In their model, Pringle and Rees assume that the accreting matter assumes a Keplerian orbit around the neutron star. They also considered the contributions of the disc gravity and relativistic effects were negligible. The radial velocity v_R can be then determined by

$$v_R = y\frac{v_{orb}}{100} \tag{2.50}$$

where y is the dimensionless viscosity parameter ~ 1 , and v_{orb} is the orbital velocity. If M is the mass of the central neutron star and R_4 is the orbital radius given in units of $10^4 cm$

$$v_{orb} \approx 1.15 \times 10^{10}(M/M_{Sun})^{1/2}{R_4}^{-1/2} m\ s^-1 \tag{2.51}$$

We can therefore find the flux F of the accreting matter by

$$F = 2\pi R \times 2b\rho v_R \tag{2.52}$$

Substituting in v_{orb} and b, ρ is determined to be

$$\rho = 1.4 \times 10^{-4} y^{-1} x^{-1} \left(\frac{M}{M_{sun}} \right) \tag{2.53}$$

where x and y are dimensionless parameters dependent on the radius R and viscosity, respectively. And the power per unit area $p(R)$ is

$$p(R) = \frac{2FGM}{4\pi R^3} \tag{2.54}$$

For a neutron star of radius R, when the accretion disc reaches the surface of the neutron star, the luminosity L of the disc

$$L \approx 7 \ \times 10^{35} \ F_{16} \ (M/M_{Sun}) \left(\frac{R}{10^6} \right)^{-1} \ ergs \ s^{-1} \tag{2.55}$$

where F_{16} is the flux given in units of $10^{16} g \ s^{-1} \approx 1.5 \times 10^{-10} M_{Sun} \ yr^{-1}$ The lower temperature limit, assuming the disc radiates like a blackbody, is the *blackbody temperature* T_{bb} which is

$$T_{bb} = \frac{p(R)}{2\sigma} \tag{2.56}$$

where σ is the Stefan-Boltzmann constant. Since this is a lower limit, this means that the temperature of the disc can be hotter if the cooling processes are not efficient enough to radiate energy at the blackbody temperature.[32]

Four Cases of Neutron Star Accretion

Neutron stars can participate in the accretion process in four different ways:

I. For neutron stars, If the mass is too large or too small, accreting matter is expelled because the radiation pressure prevents steady accretion in the first case, or the gravitational energy cannot be radiated effectively in the latter

II. The accretion disc will extend to the surface if the magnetic field of the neutron star is small enough, so it can be expected that the amount of x-rays should be similar from the neutron star and the disc.

III. For a slowly spinning magnetized neutron star, the accreting matter will follow the field lines and accrete near the poles. Therefore, X-rays should be emitted most strongly from the poles.

IV. For a rapidly rotating neutron star, or a star with a very strong magnetic field, then accretion will fail to take place, and rotational energy will be the main source of energy to the system.

For cases such as II, the dominant source of emission is *bremsstrahlung* radiation (or free-free, meaning that the radiation is generated by free particles that scatter each other) with the *bremsstrahlung temperature* $T_{ff}(R)$ at radius R

$$T_{ff}(R) = 1.1 * 10^{10} {F_{16}}^{-2} \ \frac{M}{M_{Sun}} x^2 y^4 {R_6}^{-2} K \tag{2.57}$$

Assuming the effects of electron scattering were negligible, then

$$T \approx max\left[T_{bb}, T_{ff}\right] \tag{2.58}$$

As we move further away from the central mass, T_{ff} decreases more sharply than T_{bb},

When electron scattering is significant, then the luminosity cannot exceed the *Eddington limit*, which is the maximum luminosity a star can attain when the gravitational force and force from radiation pressure is balanced. This condition is also called *hydrostatic equilibrium* When the mass flux is very large, the disc will become almost spherical and the mass will fall radially inward without radiating much energy.

The inner section of the disc has to meet criteria 1 and 3 to maintain accretion

$$R_6 = 0.6F_{16}x^{-1} \tag{2.59}$$

$$T \leq T_{max} = 2.4 \times 10^9 \frac{M}{M_{Sun}} {R_6}^{-1} x^2 K \tag{2.60}$$

$$R_6 \geq 5F_{16}x^{-2}(\frac{M}{M_{Sun}})^3 y^4 \tag{2.61}$$

Or, when the gravitational influence of the accreting star becomes significant.

If the neutron star does not have a magnetic field, then the innermost radius will extend to the surface of the neutron star.

For our purpose, it is desirable to look at neutron binary accretion during quiescence, that is, the duration through which neutron star activity is at its lowest level- because it simplifies the analysis by ignoring thermonuclear bursts.

Neutron Star Accretion at Low Eddington Rates

Degenaar,et al. [10] describe observations of neutron stars accreting at low Eddington rate using data from $NuSTAR$, $Swift$ *and* $Chandra$ [**?**] [40] [9]

observations of the low-mass X- ray binary $IGRJ17062-6143$ to study low mass X-ray binaries with long accretion period[10].

Low mass X-Ray binaries (LMXBs) are compact systems (such as a neutron star or black hole) that accrete matter from a lower mass star. As the accretion process persists, X-rays are emitted over a wide range of luminosities.

The X-ray luminosity L_x occurs at various rates. However , they can be most readily observed when $L_x/L_{Edd} > 0.1$, where L_{Edd} is the Eddington luminosity. Additionally, the accretion that leads to the emission of X-rays may occur during relatively quiet periods which we call quiescent periods. While LMXB's spend only a short time in the quiescent phase, there are nearby neutron stars which remain in this phase over an extended period, sometimes for as long as several years. These kinds of X-ray binaries, called very faint X-ray binaries (VFXBs), are good candidates in order to study how low level accretion takes place.

It has been observed that for neutron stars, when $L_x > 0.01\ L_{Edd}$, matter in the inner accretion disc may evaporate into a hot accretion flow, which will inhibit the accretion efficiency. As a result, the X-rays emitted are less energetic when L_x is in the range of $0.0001\ L_{Edd}$. However, this energy is small when compared to the thermal energy from resulting from matter heated by the neutron star's surface as it is being accreted. The authors of this paper therefore construct models using several codes to determine whether this is the case or not, and ascertain the consequences.

Currently, the disc instability model of accretion would suggest that these low accretion flows should not be stable for the relatively long periods we

observe them. One explanation for this is that low rate of accretion stability may be maintained if the neutron star has a sufficiently strong magnetic field that slows accretion.

When the authors looked at spectral data from $NuSTAR/Swift$ [**?**] [40] from $IGRJ17062-6143$ in the $.5-79\ keV$ range, they observed that a broadened iron-potassium line $\sim 7\ keV$, which is common in LMXB that are more luminous. This seems to suggest that the innermost section of the accretion disc truncated at some distance away from the innermost stable circular orbit (ISCO).

From the *Chandra* data [9] [29], emission lines of 12 Angstroms are observed at $\sim 1\ keV$ that may be modelled as reflection spectra or possibly plasma that is ionized due to collisions. In addition, at $\sim .77\ keV$, a broad 16 Angstrom absorption line is observed that can be modelled as an photo-ionized plasma outflow. These results together seems to support two ideas. Either the inner accretion disc is truncated by inefficient flows near the surface of the neutron star, or the magnetosphere is acting as a propeller directing the accreting matter toward the poles. Furthermore, if the flow inhibited in this manner, this constrains the spin period and the strength of the magnetic field.

CHAPTER III:

NEUTRON STARS

Neutron stars are highly degenerate compact objects that are believed to form when a massive star $\sim 8-30\ M_{Sun}$ goes supernova, which occurs when a star gravitationally collapses after it has expended its nuclear fuel. The have a mass between 1-4 solar masses and a radius no greater than 15 km. Astronomers Walter Baade and Fritz Zwicky were the first to hypothesize the existence of neutron stars [2]. They also proposed that such objects might form from supernovae (which is now the current consensus).

Five years later, J Robert Oppenheimer and George Volkoff were able to determine a possible interior structure of a neutron star by solving the relativistic equations of a neutron gas [28]. This was accomplished by assuming the degenerate neutrons behaved as an ideal gas at high density. At the time, most work on neutron stars was oriented toward the notion that neutron cores may be a source of energy for stars [35]. Unfortunately, the astronomical community moved away from this research until the late 1960s.

However, this changed with the discovery of cosmic radio sources by Giacconi et al. in 1962 [12]. Schmidt, however, would discover, in 1963, the presence of the first quasi stellar object (QSO)[36]. As a result of these discoveries, theoreticians began to focus on the properties of neutron stars in equilibrium and on stellar collapse [35], but the astrophysics community at large still did not seriously entertain the idea that these objects actually existed. With the discovery of pulsars in 1967, and Tommy Gold's proposal

that these pulsars were rotating neutron stars, the general acceptance of the existence of neutron stars was established [13].

In the following sections, we will discuss the structure of neutron stars, the equation of state (and perhaps ways to obtain a more realistic equation of state experimentally), the types of neutron stars, and possible objects that may form when neutron degeneracy pressure is exceeded (but not yet lead to total gravitational collapse).

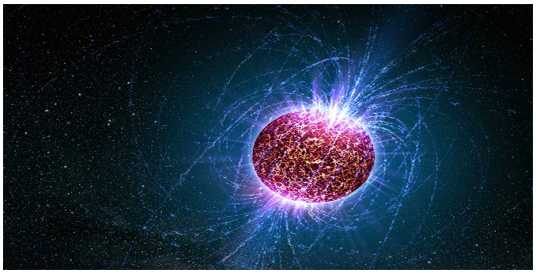

Figure 3.1: An artist depiction of pulsar type neutron star.
Source:`https://www.skyandtelescope.com/astronomy-news/magnificent-neutron-star-found`

Structure of Neutron Stars

The structure of matter at the densities found in neutron stars is of paramount interest to physicists, and, currently, is an unresolved problem in modern physics [43]. Matter at the core of neutron stars is compressed much more tightly than the density of atomic nuclei. Therefore, we expect exotic forms of matter not seen in 'normal' circumstances.

If there are an equal number of protons and neutrons, there are various observational constraints at the saturation density. Since we cannot directly observe neutron star cores, we instead try to look at macroscopic properties

such as the mass, radius, charge, or temperature to infer other properties which are not as easily determined.

These properties will allow us to ascertain or at least constrain the equation of state (EOS). In the astrophysical context, the equation of state will allow us to understand events like binary mergers and gravitational wave signals.

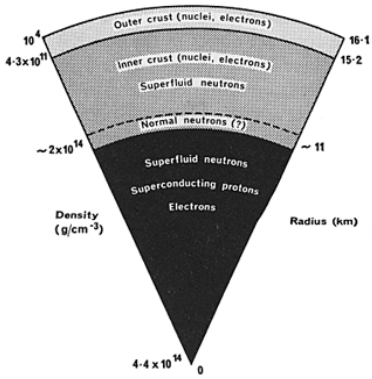

Figure 3.2: Internal structure of neutron star. Source: `https://heasarc.gsfc.nasa.gov/docs/objects/binaries/neutron_ltar_structure.html`

Nucleonic (protons and neutrons) interaction govern the properties of neutron stars. Oppenheimer and Volkoff [28] demonstrated that if the neutron star is composed of non-interacting neutrons, the maximum mass of the star is $0.7M_{sun}$. This entails that the nucleons inside neutron stars must exert a repulsive force. However, at low energies, the interaction between these nucleons is attractive. Two and three nucleon interactions become significant at higher densities. As a result, neutron stars are sensitive to many-body interactions [1]

At the densities inside neutron star cores, it is possible that non-nucleonic matter made from strange quarks may form. This may occur in the form

of hyperons (baryons composed of quarks other than u or d quarks), non-confined quarks, Bose-Einstein condensates or, and possibly the most exotic circumstance, the formation of a strange quark star. [34]

Neutron Star Regions

The physical structure of a neutron star consists primarily of four regions: the surface, crust, outer core, and inner core. At this point, we will discuss each region briefly

At the surface of a neutron star, there exists an atmosphere and an envelope. As the density in this region is only $\sim 10^6 g/cm^3$, the contribution to the overall mass of the star is minimal [34]. The crust has a thickness of approximately 1-2 km and is comprised of nuclei. In this region, ^{56}Fe dominates at $\rho < 10^6 g/cm^3$

At *neutron drip*, the limit which nuclear decay by emission of neutrons no longer occurs, $\rho = 4 \times 10^{11} g/cm^3$ and the chemical potential is zero. Neutron will begin to leak out of nuclei, creating a sea of disassociated neutrons. For high density matter at the core of neutrons stars, the quarks that compose the baryons may be compressed so tightly that the interactions between the quarks are weakened and therefore act as if they are free, which is called *asymptotic freedom*. Thuss the nuclear interaction is only defined for a very short range, that is sufficiently smaller than the size of the atomic nuclei.

Neutron Star Ideal Equation of State (Above Cold Neutron Drip)

In 1939, Volkoff and Oppenheimer performed the first neutron star model calculation by assuming that neutron stars behave as an ideal gas at high density. Unfortunately, we know that this is not the case, as fusion reactions are abundant in neutron stars. Setting this technical detail aside for the moment, we revisit the structure of neutron stars using the ideal equation of state for a self gravitating Fermi gas of neutrons, originally presented by Shapiro and Teukolsky [35]. In this model, the energy of the system E is expressed in terms of the Fermi momentum p_f defined by

$$E^2 = {m_n}^2 c^4 + {p_f}^2 c^2 \tag{3.1}$$

Where m_n is the neutron rest mass. The number density n can be calculated by

$$n = \int \frac{d\mathcal{N}}{d^3x d^3p} d^3p \tag{3.2}$$

where $\mathcal{N}$ and x and p are the standard 3 dimensional variables in phase space. Note here that

$$\frac{d\mathcal{N}}{d^3x d^3p} = \frac{g}{h^3} f \tag{3.3}$$

Where g is the degeneracy, h is Planck's constant, and f is an arbitrary distribution function. If the system is isotropic then the pressure P is given as

$$P = \frac{1}{3} \int pv \frac{d\mathcal{N}}{d^3x d^3p} d^3p, \tag{3.4}$$

where $v = pc^2/E$. The distribution functions of particles at energy of the system E depends on their spin statistics and are expressed as

$$f(E) = \frac{1}{exp(\frac{E-\mu_{ln}}{kT}) \pm 1} \tag{3.5}$$

Here, +1 indicates that the gas obeys Fermi-Dirac statistics, and -1 obeys Bose-Einstein statistics. For degenerate fermions ($T \to 0$ or $\mu_l/k_BT \to \infty$),

$$f(E) = \begin{cases} 1/2, & \text{if } E \geq E_f \\ 0, & \text{if } E < E_f \end{cases} \tag{3.6}$$

Therefore,

$$n_n = \frac{2}{h^3}\int_0^{p_f} 4\pi p^2 dp = \frac{8\pi}{3h^2}{p_f}^3 \tag{3.7}$$

Here, a variable substitution can be made such that

$$x = \frac{p_f}{m_n c} \tag{3.8}$$

Then,

$$n_n = \frac{1}{3\pi^2 {\lambda_c}^3}x^3 \tag{3.9}$$

Where n_n is the neutron number density λ_c is the Compton wavelength of the neutron. Therefore the neutron pressure P_n

$$P_n = \frac{2}{2h^3}\int_0^{p_f} \frac{p^2c^2}{(p^2c^2 + m^2c^4)^{\frac{1}{2}}} 4\pi p^2 dp = \frac{8\pi {m_n}^4 c^5}{3h^3}\int_0^{p_f} \frac{x^4 dx}{(1+x^2)^{\frac{1}{2}}} \tag{3.10}$$

A relatively realistic model of neutron star can be constructed based on the proper calculation of pressure. And an equation of state can be written from the rate of change of this pressure.

Realistic Theoretical Model of Equation of State

The classical stellar structure equations describe the internal structure of a self-gravitating, spherically symmetric star. While there are four equations governing stellar structure, we will only be concerned with 3 of them. These are

$$\frac{dP}{dr} = -\frac{GM_r\rho}{r^2}\ (hydrostatic\ equilibrium) \tag{3.11}$$

$$\frac{dM_r}{dr} = -4\pi r^2\rho\ (mass\ continuity) \tag{3.12}$$

$$\frac{dL}{dr} = -4\pi r^2\rho(\epsilon)\ (energy\ equation) \tag{3.13}$$

Because of general relativistic effects arising from the compactness of the neutron star, the second equation must be modified using the Einstein field equations. Thus, the hydrostatic equilibrium equation becomes

$$\frac{dP_r}{dr} = -\frac{\rho m}{r^2}\left(1+\frac{P}{\rho}\right)\left(1+\frac{4\pi Pr^3}{M_r}\right)\left(1-\frac{2M_r}{r}\right)^{-1}(mass\ continuity) \tag{3.14}$$

This equation, called the $Tolman-Oppenhiemer-Volkoff\ equation$, governs the changes in the internal pressure P of neutron stars as a function of the radius r of the star and help to determine the size of the star.

A spherically symmetric, isotropic body will maintain hydrostatic equilibrium if it is solvable under an equation of state of the form

$$P = P(\rho) \tag{3.15}$$

where P is pressure and ρ is the density of the neutron star [35].

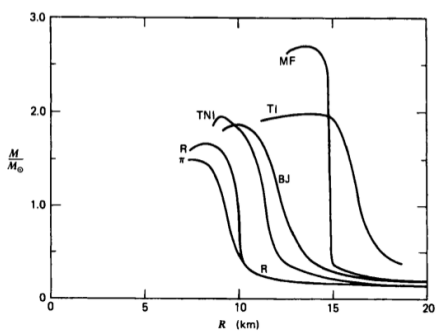

(a) Mass vs Radius

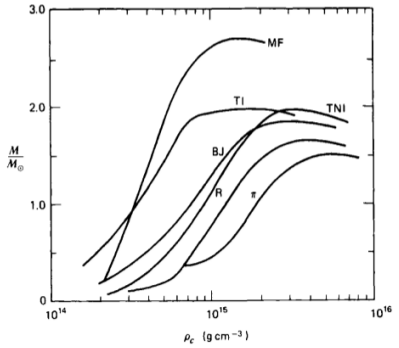

(b) Mass vs Density

Figure 3.3: (a) mass vs. radius and (b) mass vs. density for various NS equations of state. Source: [35]

However, we do not have a singular model, as the equation of state of nuclear matter can be difficult to determine. Instead, one can construct a sequence of stars with the same equation of state (EOS) but different central core densities. If we parameterize this sequence with a *critical density* ρ_c, we can determine where in the sequence of stars we achieve stability, in particular models when $dM/d\rho_c > 0$, and those with $dM/d\rho_c < 0$ are considered unstable.

It is useful for us to compare different models for the equation of state. From Table 3.1 and Figures 3.3b and 3.3a, a few trends become apparent. For 'stiff' EOSs (those for which numerical solutions to the differential equations describing them must have a small step size to be solvable), the maximum mass is greater than models with 'soft' EOSs. As a result, they have a lower central core density, a thicker crust, and a larger radius [35]. Pion condensation-which occurs when a pions under tremendous pressure occupy the lowest energy state and exhibit quantum effects on macroscopic scale-if any, also contracts neutron stars for any particular mass and limits the

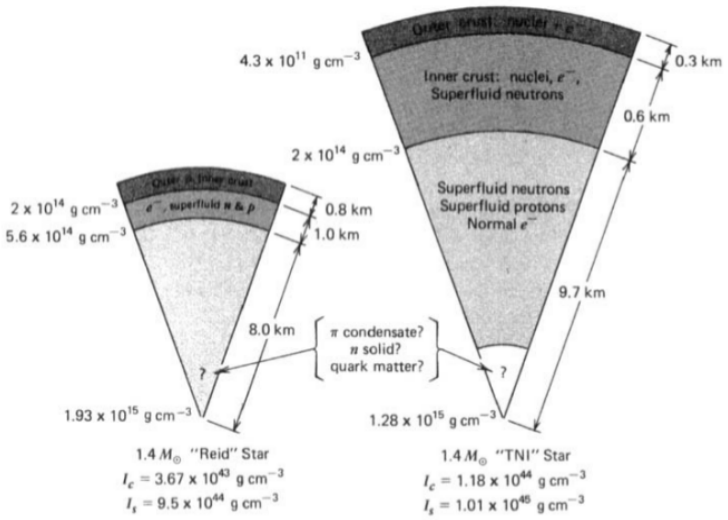

Figure 3.4: Cross sections of a 1.4 solar mass NS for Reid and TNI equations of state. Source: [35]

maximum mass.

Equation of State	Maximum Mass (M_{Sun})
π	1.5
Reid	1.6
Bethe-Johnson (BJ)	1.9
TNI	2.0
Tensor-Interacting (TI)	2.0
Mean Field (MF)	2.7

Table 3.1: Maximum masses for several equations of state model. 'Stiff' equations of state lead to larger maximum masses. Source: [3]

X-Ray Timing and Equation of State

Understanding the processes in the interiors of neutron stars can be difficult. However, it may be feasible to determine "external" properties, such as the radius of a star . This could allow us to determine the equation of state, and therefore the internal structure, of neutron stars. Watts, et. al [43], using

complementary techniques, proposed a couple of approaches to determine the equation of state.

The first part involves waveform modeling. This allows us to measure the radius of a neutron star by observing a particular area on the surface of the neutron star and notice that the flux will begin to be modulated at the star's rotational frequency, resulting in pulsation. The emissions from the surface will encode information about the radius as relativistic effects act on the photons escape the surface.

Accreting neutron stars have been observed to produced millisecond x-ray oscillations. It is believed that this happens because accreting matter striking the surface of the neutron star causes the region to heat up to a temperature that is hotter than the average temperature of the star as a whole. This region then rotates around the star near rotational frequency, which produces a modulated flux from the point of view of a distant observer. X-ray pulses may also occur as matter will tend to accrete near the poles. These pulses would allow us to glean information about the mass and radius of the accreting neutron star.

Since neutron stars are so dense, we can expect general relativistic effects, which depend on the compactness (the ratio of the mass to the radius), and special relativistic effects which arise from the orbital velocity, to affect the waveform. These effects depend on the ratio

$$\frac{f_s}{f_0} = .24\left(\frac{f_s}{600Hz}\right)\left(\frac{M}{1.8M_{sun}}\right)^{-1/2}\left(\frac{R}{10km}\right)^{3/2} \tag{3.16}$$

where f_s is the frequency of the spin of the neutron star and $f_0 = \sqrt{\frac{GMR^3}{2\pi}}$is the fundamental frequency. An expansion of this function with respect

to f_s will describe a spherically symmetric neutron star with an external Schwarzschild spacetime metric in the zeroth order, the Kerr model in the first order, and the Hartle-Thorne model in the second order. In the first order, the amount of gravitational lensing depends not only on the mass, but the angular momentum of the star. Therefore we can determine facts about the density profile of the star, which also depends on the equation of state.

Secondly, we can look at the distribution of spin in the neutron star by looking at the pulsations while it is accreting. The maximum spin frequency is a function of the neutron star mass and radius and is determined by

$$f_{max} \approx C\Big[\frac{M}{M_{sun}}\Big]^{1/2}\Big[\frac{R}{10km}\Big]^{-3/2} kHz \tag{3.17}$$

The radius is therefore limited to

$$R < 10\ C^{2/3}\Big[\frac{M}{M_{sun}}\Big]^{1/3}\Big[\frac{f_s}{1kHz}\Big]^{-2/3} km \tag{3.18}$$

The parameter C, for a hadronic equation of state under general relativistic effects, depends on neutron star's mass distribution and is determined to be 1.08 (the Newtonian value is 1.838). Therefore, fast spinning neutron stars would constrain the equation of state.

In conclusion, using the waveform and spin distribution will allow us to understand what goes on in the interiors of neutron stars. Despite not having a clear understanding of the structure of the interior, quantities such as the radius, mass, and spin distribution constrain the equation of state.

Types of Neutron Stars

X-ray Binaries

X-ray binaries are binary systems that contain a primary neutron star or black hole accretor and a non-compact companion star that accretes onto the primary. As a result of the accretion process of the primary, the system will radiate X-rays. While a few hundreds of these binaries are thought to exist, relative to the estimated abundance of stellar mass black holes (10^8), this would make X-ray binaries quite rare.

These can be classified into two distinct categories: low mass X-ray binaries (LMXBs) and high mass X-ray binaries (HMXBs). These two classes of binaries account for around 90% of galactic x-ray sources [34]. LMXBs and HMXBs are thought to come from different stellar populations, for the reason that LMXBs have a slowly evolving low mass companion and HMXBs have a young, massive companion and are located near the spiral arms in the galactic plane. In the next sections, we will describe each one of them in a little more detail.

High Mass X-Ray Binaries

High mass X-ray Binaries (HMXBs) occur when the donor star has a mass greater than 10 solar masses. In high mass x-ray binaries, matter falls onto the surface of the compact star (called an accretor) through transfer by stellar winds from the donor star driving matter in the direction that are ultimately captured by the gravitational pull of the compact star [21]. This occurs when the companion fills its Roche lobe completely until matter is able to escape

to accrete onto the primary in a process called *Roche lobe overflow*.

In HMXBs, the optical source of photons tends to be the supergiant companion, while source of X-rays is the result of gravitational potential energy being released as matter accretes onto the primary. Most HMXBs discovered thus far are Be/X-Ray binaries [25], meaning that the companion star is a B-class star with emission lines. Since the lifetime of these types of stars are limited, they tend to be found near the star-forming regions in the Galactic Disc [34]. As of 2007, about 130 HMXBs have been discovered [19]

Approximately half of HMXBs have pulsation cycles from 10-300 seconds. Orbital periods can range from a few hours to hundreds of days Strong X-ray sources, such as Cen X-3 and SMC-1, are characterized by periodic X-ray eclipses and double wave ellipsoid light variations as a result of tidally deformed subgiant companion stars with M $>$ 10 solar masses [41]. From Table 1, we can see that the X-ray spectra tend to be hard (high energy with E $\geq$ 15 keV) with the accreting neutron star or black hole having a high magnetic field.

Low Mass X-Ray Binaries

In the case of LMXBs, a smaller star accretes onto the compact star when the donor star encroaches within a critical distance of the compact object. At this distance, called the Roche limit, a disc will form around the accreting compact stars that channels matter onto the compact star. In this scenario, the donor star is less massive than the accretor. The companion of a LMXB is usually less than 1 solar mass. The types of companions in an LMXB may be white dwarfs, late main-sequence stars, A, and F-G subgiants [19]

	HMXB	LMXB
X-ray spectra	kT $\geq$ 15 keV (hard)	kT $\leq$ 10 keV
Type of time variability	regular X-ray pulsations no X-ray bursts	only a very few pulsars often X-ray bursts
Accretion Process	wind (or atmos. RLO)	Roche-lobe overflow
Timescale of Accretion	10^5 years	$10^7 - 10^9 yr$
Accreting compact star	high B field NS (or BH)	low B-field NS(or BH)
Spatial Distribution	Galactic plane	Galactic center and spread around the plane
Stellar Population	young age $< 10^7$ years	old age $> 10^9 yr$
Companion stars	luminous, $L_{opt}/L_x > 1$ early type O(B) stars $> 10 M_{Sun}$ (Pop. I)	faint, $L_{opt}/L_x << .1$ blue optical counterparts $\leq 1 M_{Sun}$ (Pop I and II)

Table 3.2: Classification of the two main X-Ray Binary Types. Source [41]

From observed LMXBs, the orbital period for these systems can range anywhere from 11 minutes to 17 days. Because the companion is not very luminous due to its size, oftentimes the optical spectrum of the companion is not observable. Instead, the optical component of the binary is the result of the accretion disc that is formed around the primary. Unlike HMXBs, LMXBs have a relatively weak magnetic field (only $10^9 - 10^{11} G$), and thus are not likely to be X-ray pulsars (discussed in the next section). LMXBs tend to be 'soft' sources of X-rays with energies less than 10 keV.

LMXBs are located in globular clusters and in the Galactic bulge, and are therefore believed to be older systems. While some have velocities in excess of 100 km/s, those in globular clusters must have velocities of less than 30 km/s to remain bound to them [41]

Pulsars

Jocelyn Bell Burnell and Anthony Hewish would later make the first observation of an extrasolar source that exhibited regular pulsations. Burnell and Hewish eventually found three more of these sources, called pulsars, and were theorized to be rotating neutron stars with a very strong magnetic field. This discovery led to the awarding of the 1974 Nobel Prize to Hewish along with Martin Ryle.

Locating Pulsars

Pulsars tend to be located most often in the galactic disc [34]. We can give a rough estimate of the distance to a pulsar by its pulse dispersion. Since pulses with higher group velocities will arrive at a detector here on Earth earlier than pulses with longer wavelengths, we can show the period between the arrival of signals as a function of the distance

$$\Delta t = 4150s \left(\frac{1}{{v_{low}}^2} - \frac{1}{{v_{high}}^2} \right) \rho_D \tag{3.19}$$

where ρ_D is the *dispersion measure*, which is effectively the intensity of the signals as a function of distance x, is defined as

$$\rho_D = \int_0^d n_e(x) dx \tag{3.20}$$

where d is the distance from the observation position to the pulsar and n_e is the electron number density along the line of sight.

While this calculation is model dependent with respect to the distribution of free electrons, it provides a reliable estimate of the distance within a factor

of two [34].

Are Pulsars Neutron Stars?

Pulsars have properties that lead us to believe that they are indeed neutron stars. For one, they have short rotational periods ($P \sim 1.5$ ms)that may slowly increase $\left(\frac{dP}{dt} \sim 10^{-15} s^{-2}\right)$. Lastly, the signal they emit is very regular, and therefore be used as a "clock" [34]. We can therefore deduce other characteristics based on these properties.

Consider a source with diameter D_s. If it emits a signal with period τ, then by mere mechanics, $D_s < c\tau$. If we assume $\tau = 1.5$ ms, then

$$D_s < c\tau = (3.00 \times 10^8 m/s)(1.5 \times 10^{-3} s) = 450 km \tag{3.21}$$

This is much smaller than a white dwarf of a mass approximately the Chandrasekhar limit, the maximum allowable mass of a stable white dwarf($\approx 1.4 M_{Sun}$). Additionally, since it is improbable that black holes will emit signals with the intensity observed, this leads us to suspect neutron stars as the most likely source.

Pulsation or Rotation?

If we assume neutron stars pulsate with a period of approximately that of the dynamic timescale $\tau_d \approx 10^{-3}$ s

$$P \approx \tau_d = \frac{1}{\sqrt{G\rho}} \tag{3.22}$$

where G is the gravitational constant and ρ is the mean neutron star density. Rearranging and taking the pulsation period

$$\rho = \frac{1}{\sqrt{GP^2}} \approx 7 \times 10^{12} \frac{g}{cm^3} \tag{3.23}$$

which is about 100 times less than the average known density of neutron stars.

If we consider rotation, the maximum rotation occurs when the gravitational force of the star dominates the centrifugal force on a mass element on the surface [34]. If we equate the angular acceleration at the surface we obtain

$$\frac{d\omega}{dt} = G\frac{M}{R^3} = G\frac{4}{3}\pi\rho \tag{3.24}$$

Thus,

$$\rho = \frac{3\pi}{GP^2} \tag{3.25}$$

Here, P is the rotational period of the neutron star. The density ρ is a lower limit on the real average density [34]. Again letting P = 1.5 ms, the average density for a neutron star is $\approx 6 \times 10^{13} g/cm^3$.

Magnetars

Magnetars are a class of neutron stars which is highly magnetized and is variable across its entire spectrum. This may manifest as shot bursts, large bursts, giant flares, and quasi-periodic oscillations [15]. the activity is best explained by the formation and decay of very strong magnetic fields. As these fields form and collapse, this causes the crust to stress and break, which in turn affects the magnetosphere and drives energetic magnetic currents. In

the following subsections, the basic properties and behaviors of magnetars will be discussed.

Properties of Magnetars

The catalogue of Olausen and Kaspi [27] has a compendium of the 30 known magnetars and their respective properties given in Table 2.1. The majority of the known magnetars have been found by detecting short X-ray bursts in surveys such as the $Swift\ Burst\ Alert\ Telescope$ and the $Fermi\ Gamma-ray\ Burst\ Monitor$.[40] [11]

While our current methods of observations seem to bias toward the detection of magnetars that are likely to burst, it has been shown that currently the magnetars share common properties such as the emission of X-rays and gamma rays, and a magnetic field $\simeq 10^{15}G$ [27]

Magnetars are observed to have X-ray pulsations $\simeq 2-12\ seconds$. Magnetars, without exception, are spinning down, with the spin-down time scales of order of a few thousand years. These spindown rates also imply that the magnetic field $B > 10^{13}$ Gauss with the majority having $B > 10^{14}G$. unlike other kinds of neutron stars, magnetars are generally thought to have longer rotational periods despite being young (young neutron stars tend to have 1 ms or even sub-millisecond rotational periods)

On the other hand, there is a wide range for the X-ray luminosity from $10^{30} - 10^{35} ergs\ s^{-1}$ in the 2-10 KeV band [15]. The quiescent (quiet) luminosities seem to be grouped into two categories: Brighter magnetars which are "persistent", and the fainter magnetars are "transients".

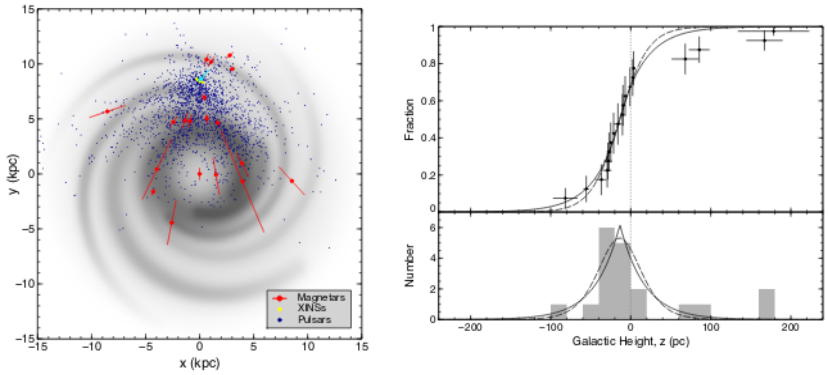

Figure 3.5: On the left:top down view of the galaxy showing the locations of known magnetars (in red) On the right: The fraction of magnetars at particular z-heights from the galactic plane. Source: [15]

Where are Magnetars Located?

As with other types of neutron stars, magnetars are confined to the disc of the galaxy, with a scale height of 20-30 parsecs. The scale height is in this context is the length in which particular features drop by a factor of e. the spacial velocity is approximately 200 km/s. This would indicate that at most, magnetars are $\sim 10^5$ years old.

Exotic Stars

While neutron stars, under 'normal' circumstances, collapse into black holes once they exceed the $Tolman-Oppenheimer-Volkoff$ (TOV) limit, there are some hypothetical states which may be achieved under special conditions. These types of stars, called exotic stars, represent a theoretical frontier that isn't well understood. While quark stars, a subclass of exotic stars, are the best understood and has the strongest evidence supporting their existence, other types such as strange stars and preon stars are also possibilities.

Although this isn't the focus of this research, it may be useful to briefly discuss the different types of exotic stars, as they may possibly be an end result of magnetic collapse, or magnetic collapse may be a prelude or requirement for these stars to form.

Quark Stars

Quark Stars are an exotic star class where neutrons are compressed so tightly under extremely high temperatures and pressures that a state of "free" quarks forms.

Depending on the temperature and chemical potential, we can expect two regimes under which conditions occur naturally. The first of these ($T >> \mu_l$) is the 'hot' phase and would have been present the first few seconds after the Big Bang. In this kind of plasma, the quarks are close enough together that they are asymptotically free. This is called a quark-gluon plasma.

The other regime occurs when $T << \mu_l$ and is expected in the interiors of neutron stars. In these stars, neutron matter is thought to undergo a phase transition where u- and d-quarks absorb electrons and neutrinos to produce s-quarks.

Preon Nuggets

Preon nuggets are hypothetical objects composed of preons, a hypothetical particle that form the substructure of quarks and leptons first suggested by Hansson and Sandin in 2005 [14]. Preons nuggets are believed to be compact objects that are unable to survive as neutron stars, yet stable enough to not collapse into black holes. Asymptotically free fermions in QCD put an upper

limit on which kinds of compact objects can exist stably under the Standard Model and stellar structure equations, new physical models superseding the Standard model will be necessary in order to explore this regime.

Structure and Stability of Preon Nuggets

It is necessary, like all other compact objects, that preon nuggets have a total mass that is a function of the central core density and is also stable to radial oscillations.

Preon nuggets are expected to be very small ($10^{-1} - 10^{-4}m$). Primordial preon 'nuggets' may have possibly formed in the early universe (Hansson and Sandin). These preons would not have taken part in big bang nucleosynthesis and also would not evaporate via Hawking radiation. That is why they failed to attract enough attention of astrophysicists and were not easily observable either.

Preon nuggets are also a possible candidate for dark matter in galaxies. Given that 4% of the total mass of the universe is in the form of luminous matter. Let us assume that the dark matter density $\rho_{DM} = 10^{-25} g/cm^3$, then we expect the number density of preon stars to be 10^4 per cubic parsec [14]. In principle, it should be possible now to detect preon stars using gravitational microlensing.[14]

CHAPTER IV:

QUANTUM MAGNETIC COLLAPSE

Under certain conditions, a relativistic neutron gas in a magnetic field (such as a neutron star) may experience anisotropic pressures parallel and perpendicular to the magnetic field generated by the constituent charged particles [8] . The pressure transverse to the magnetic field can be less than that of the pressure parallel to the field. This phenomena, called quantum magnetic collapse (QMC), describes the dynamical behavior of a massive star and is related to its stability. A star at the limit of QMC can result in stellar remnants such as a strange star - a star composed of strange quarks - or an oblate black hole [22].

This collapse can be expected to occur when the magnetic energy is of the same order as the internal energy. Since it is the case that magnetic collapse is at the stability limit of degenerate systems, the nature of the phase transitions would seem to suggest that new physics is necessary to explore this phenomena further.

At this point, we will take the time to discuss the specific conditions needed for quantum magnetic collapse. In particular, we assume that the neutron "gas" has a background of neutrons and protons in thermodynamic equilibrium, which is needed for neutron stability [22]. This necessarily means that there are equal numbers of positive and negative charges so that the system in consideration is electrically neutral. In addition, the spins of the particles of each species are coupled with the magnetic field B. We also

assume that the external B-field is uniform.

A calculation scheme for the particle number for each of the species of leptons and bosons, which we are concerned with, will be developed in the following sections. By virtue of the fact that gases are multiparticle systems, quantum statistical mechanics will need to be employed to examine the family of leptons and bosons relevant to the effect. Considering the leptonic component of the energy (electrons and positrons) requires employing Fermi-Dirac statistics in the grand canonical ensemble, and Bose-Einstein statistics when we consider the bosonic component.

The Conditions of Quantum Magnetic Collapse

In order to understand how quantum magnetic collapse occurs, it is important to know how much the lepton and quark families each contribute to the generation of the magnetic field, and therefore the contribution to the energy density (or pressure) along the magnetic field and perpendicularly to the magnetic field. Since particles and energy are being exchanged, the grand canonical partition function is most appropriate to calculate the particle number density. As a background assumption, we consider leptons and quarks are in chemical equilibrium. It is also important to note which regime is being considered, whether it be in the astrophysical or cosmological case. In the cosmological regime, we expect bosonic sectors to be significant due to the energy scales involved, whereas in the the astrophysical context, the leptonic sectors will dominate [8][22] Let us define Z as the grand canonical partition function for leptons and bosons with

$$Z = (1 \pm \exp(-\beta(E - \mu_l))(1 \pm \exp(\beta(E - \mu_l)) \tag{4.1}$$

where $\beta = T^{-1}$ (or kT in SI units), E is the average energy particle species l, and μ_l is the chemical potential of the particle species l. This expression takes into consideration the first and second terms of this product corresponds to the spin up and spin down contributions of the particle species, respectively.

The thermodynamic potential Ω is the energy per unit volume for both leptons and bosons is defined as $\Omega = -T \ln Z$. where Z is the grand canonical partition function and T is the temperature. Here, the potential is the sum of the Helmholtz free energy from electrons and the W bosons ($\Omega = \Omega_l + \Omega_b$). If we consider the lepton/anti-lepton component of Ω as $\Omega_l = \Omega_{sl} + \Omega_{0l}$, where

$$\Omega_{sl} = -\frac{eB}{4\pi^2}\sum_0^\infty a_n \int_{-\infty}^{\infty} dE \, \ln\left[(1 + e^{-(E-\mu_l)\beta})(1 + e^{-(E-\mu_l)\beta})\right] \tag{4.2}$$

where B is the magnetic field, $E = \sqrt{p^2 + {m_l}^2 + 2(n+1)eB}$ is the energy per particle where p is the pressure parallel to the magnetic field, an m_l is the mass of the lepton. The factor a_n is the degeneracy factor where $a_n = 2 - \delta_{0N}$

For the bosons, $\Omega_b = \Omega_{sb} + \Omega_{0b}$, where

$$\begin{aligned}\Omega_{sb} = &\frac{eB}{4\pi^2}\sum_0^\infty \int_{-\infty}^{\infty} dE_{0q} \, \ln\left[(1 - e^{-(E_{0q}-\mu_b)\beta})(1 - e^{-(E_{0q}-mu_b)\beta})\right] \\ &+\frac{e\hbar cB}{4\pi^2}\sum_0^\infty b_n \int_{-\infty}^{\infty} dE \, \ln\left[(1 + e^{-(E-\mu_b)\beta})(1 + e^{-(E-\mu_b)\beta})\right]\end{aligned} \tag{4.3}$$

where the degeneracy $b_n = 3 - \delta_{0n}$. The thermodynamic potentials in both cases diverge. However, what we are most interested in is calculating the particle number, and the magnetization. In the following sections, we will develop a scheme to calculate the particle number density without having to

calculate the energy density directly.

Calculating Mean Particle Density and Magnetization

Ideally, we would like to be able to compute the thermodynamic potential in order to determine quantities such as the magnetization. However, the integrals for the thermodynamic potential discussed in the previous chapter diverge in the domain under which they are considered. Computing the mean number density, on the other hand, is a much more tractable task. Therefore, we will proceed to do so for the relevant bosons and leptons in quantum magnetic collapse. We will work in the limit which is most relevant to us, where $\mu_l >> T$ (as the case is in neutron stars). To determine the mean number density N_l, we will first consider the 'static' case, then generalize to the accreting binary case. To do this, we will need to determine the chemical potential at time t by examining how the total mass and energy change as a function of the time.

For our treatment, we will be using natural units for $Planck's\ constant\ \hbar$, the speed of light c, and the Boltzmann constant k_b where $\hbar = c = k_b = 1$

Calculating Particle Number for Leptons

We will utilize the technique developed by Masood [24]. Starting with the leptons, we will begin with the Fermi-Dirac distribution and assume that the positron contribution to this is low. Let us define the particle number for the leptons N_l by integrating the number density n_l as

$$N_l = \int_0^\infty d^3p\ n_{l\pm} = 4\pi \int_0^\infty dp\ p^2 n_{l\pm} \tag{4.4}$$

In this representation, the integration is over p, covering the entire momentum space volume. Instead, we would like to do a change of variable from p to E. For the energy

$$E^2 = p^2 + {m_l}^2 + eB(2n+1) \tag{4.5}$$

In the limit that E is sufficiently larger than the electron mass and the magnetic field such that $E^2 >> eB >> m_l$, we can binomial expand to obtain

$$N_l = 4\pi \int_0^\infty dE\ E^2 \left(1 - \frac{{m_l}^2}{2E^2} - \frac{eB(2n+1)}{2E^2}\right) n_l \tag{4.6}$$

Here, we take $n_{l\pm}$ as the antilepton and lepton particle densities, respectively, as

$$n_{l+} = (e^{\beta(E+\mu_l)} + 1)^{-1} = \sum_1^\infty (-1)^n e^{-n\beta(E+\mu_l)} \tag{4.7}$$

$$n_{l-} = (e^{\beta(E-\mu_l)} + 1)^{-1} = \sum_0^\infty (-1)^n e^{-n\beta(E-\mu_l)} \tag{4.8}$$

The integrals can be broken up into a linear combination and solved individually

$$N_{l\pm} = 4\pi \left[\int_0^\infty dE\ E^2 n_{l\pm} - \frac{{m_l}^2}{2}\int_0^\infty dE n_{l\pm} - \frac{eB(2n+1)}{2}\int_0^\infty dE n_{l\pm}\right] \tag{4.9}$$

where $n_{l\pm} = n_{l-} - n_{l+}$ is defined as the net lepton contribution The solutions to each integral can be obtained from the a, c, and d functions from Masood[23]. In the current case, when $\mu_l >> T$, the first integral becomes

$$\int_0^\infty dE\ E^2 n_{l\pm} = \frac{2}{\beta^3} d(m_l\beta, \mp\mu_l) + \frac{2m_l}{\beta^2} c(m_l\beta, \mp\mu_l) + \frac{{m_l}^2}{\beta} a(m_l\beta, \mp\mu_l) \tag{4.10}$$

where

$$d(m\beta, \mp\mu_l) = \frac{\mu_l^3 - {m_l}^3}{3{m_l}^3} - \sum_{k=0}^{\infty} \frac{(-1)^k}{\mu_l^k} \sum_{n=1}^{\infty} \frac{(-1)^n}{(n\beta)^k} e^{-n\beta(m_l - \mu_l)} \tag{4.11}$$

$$c(m\beta, \mp\mu_l) = \frac{\mu_l^2 - {m_l}^2}{2{m_l}^2} - \sum_{k=0}^{\infty} \frac{(-1)^k}{\mu_l^k} \sum_{n=1}^{\infty} \frac{(-1)^n}{(n\beta)^k} e^{-n\beta(m_l - \mu_l)} \tag{4.12}$$

$$a(m_l\beta, \mp\mu_l) = \frac{\mu_l - m_l}{m_l} - \sum_{k=0}^{\infty} \frac{(-1)^n}{(n\beta)^{1-k}} e^{-n\beta(m_l - \mu_l)} \tag{4.13}$$

Therefore

$$\int_0^\infty dE n_{l\pm} = \frac{1}{\beta} a(m_l\beta, \mp\mu_l) = \frac{1}{\beta} \left(\frac{\mu_l - m_l}{m_l} - \sum_{k=0}^{\infty} \frac{(-1)^n}{(n\beta)^{1-k}} e^{-n\beta(m_l - \mu_l)} \right) \tag{4.14}$$

In the limit where μ_l is large, the summation for all of these integrals vanishes, and, if we assume that the antileptonic contribution to the particle number $< N_{l+} >= 0$ we are left with this for the final expression for the leptonic number

$$\begin{aligned} N_{l-} = \frac{4\pi\mu_l}{\beta m_l} \left[\frac{\mu_l^2}{3\beta^2 {m_l}^2} \left(1 - \frac{{m_l}^3}{\mu_l^3} \right) + \frac{\mu_l}{\beta} \left(1 - \frac{{m_l}^2}{\mu_l^2} \right) + m^2 \mu_l \left(1 - \frac{m_l}{\mu_l} \right) \right] \\ - \frac{4\pi\mu_l}{\beta m_l} \left[{m_l}^2 \mu_l \left(1 - \frac{m_l}{{\mu_l}^2} \right) + eB\mu_l \right] \end{aligned} \tag{4.15}$$

In the limit that $m_l << T << \mu_l$, the $\frac{m_l}{\mu_l}$ terms are ignorable

$$N_l = \frac{4\pi\mu_l}{\beta m_l} \left[\frac{\mu_l^2}{3\beta^2 {m_l}^2} - \frac{eB{m_l}^2}{\beta\mu_l^2} \left(1 - \frac{m_l}{\mu_l} \right) \right] = \frac{4\pi\mu_l^3}{{m_l}^3} \left[\frac{1}{3\beta^3} - \frac{eB{m_l}^2}{\beta\mu_l^2} \left(1 - \frac{m_l}{\mu_l} \right) \right] \tag{4.16}$$

In the astrophysical context, we assume that the lepton number is dominant over the antilepton component, and that the type lepton that we are interested in is the electron. Dividing this expression by the lepton mass m_l, we will obtain the expected electron number in the neutron star.

$$N_{le} = \frac{4\pi\mu_l^3}{{m_l}^3}\left[\frac{1}{3\beta^3{m_l}^3} - \frac{eB}{\beta{m_l}^3}\left(\frac{{m_l}^2}{\mu_l^2}\right)\left(1 - \frac{m_l}{\mu_l}\right)\right] \tag{4.17}$$

It should be noted that this result, while primarily concerned with electron particle number, is generally true for all leptons. From 4.17, the particle number N_e is directly related to the chemical potential μ_l, the temperature T, and the external magnetic field B. In the limit that $\mu_l >> m_l$, the magnetic component to the particle number is dominant. When $\mu_l = m_l$, the particle number does not depend on the magnetic field, and is only a function of the mass.

Vanishing Pressure

Standard electroweak theory places an upper limit on the magnetic field generated by the accelerated charged marticles as essentially a function of their mass. If we consider the electrons, for example, the average energy E in the ground state is

$$E = \sqrt{(p)^2 + (m_l^2)^2 - (2n+1)eB} \tag{4.18}$$

where p is the pressure parallel to the magnetic field B, m_l is the mass of the lepton (in this case we are considering electrons), and e is the electron charge.

In the ground state and as the pressure p vanishes, this becomes

$$E_{0s} = \sqrt{(m_s c^2)^2 - eB} = 0 \tag{4.19}$$

Also, the total energy of the system is determined by comparing the energy of the boson plus the magnetic energy, therefore, in natural units, the critical value of the magnetic field B_c is

$$\frac{m_s^2}{e} = B_c \tag{4.20}$$

for the proton, $B_c \sim 10^{24}$ G. Performing the calculation for the magnetic field corresponding to the electron mass, $B_c \sim 10^{14}$ G.

Utilizing results from Landau and Lifschitz [18], the pressures $p_\parallel$ and $p_\perp$ can be found from the energy momentum tensor $\mathcal{T}_{\mu_l \nu} =< \mathcal{T}_{\mu_l \nu} >$ and taking the statistical average of the Lagrangian [8] [33], the longitudinal and transverse pressures are

$$p_\parallel = -\Omega \text{ and } p_\perp = -\Omega - B\mathcal{M} \tag{4.21}$$

where B is the magnetic field and $\mathcal{M}$ is the total magnetization. Note that in the above scenario, the transverse pressure is more than the pressure parallel to the magnetic field. This can lead to a "squeezing" of neutron stars.

When the magnetization is positive, the pressure transverse to the magnetic field is smaller than the pressure $p_\parallel$ by an amount $B\mathcal{M}$. In the limit where the external magnetic field is very strong $eB >> T^2$, the electrons are confined to the Landau ground state n = 0. At these energy densities, the vacuum term is ignorable, therefore

$$p_\perp = 0 \rightarrow \Omega_e = -B\mathcal{M}_e \tag{4.22}$$

If we consider a local region in a neutron star where the charge is dominated by electrons, this may lead to a collapse of the neutron star.

CHAPTER V:

DYNAMIC LEPTON NUMBER IN ACCRETING NEUTRON STARS

Determining the Dynamic Particle Number

At this point, we would like to determine the particle number and magnetization as a function of time by considering how many particles are added to the neutron star as it accretes matter from the donor star. For our purpose, we will be considering the astrophysical scenario whereby the dominant contribution to the particle number will come from ionized hydrogen. As a consequence, we are primarily concerned with the increase in particle number from electrons as the neutron star accretes. In the static case, for electrons, we can simply take the particle number $N_l = N_{e0}$ as the initial number of electrons which we are considering using Eq 4.17, which is our particle number for the electrons in the static case.

$$N_{0e} = \frac{4\pi\mu_l^3}{{m_l}^3}\left[\frac{1}{3\beta^3{m_l}^3} - \frac{eB}{\beta{m_l}^3}\left(\frac{{m_l}^2}{\mu_l^2}\right)\left(1 - \frac{m_l}{\mu_l}\right)\right] \tag{5.1}$$

However, since the neutron star is accreting, the total number of particles composing the neutron star changes with time and the initial concentration can be expressed as

$$N_e \equiv N_e(t) \tag{5.2}$$

Therefore, if we have some initial number of particles in the neutron star, then the change in the number of particles at time t becomes

$$N_e(t) = N_{e0} + \delta N(t) \tag{5.3}$$

where $\delta N(t)$ is the change in the particle number as a function of time.

Now consider the accreting matter stream. The amount of energy that each particle has is only dependent on the kinetic energy and the gravitational mass, since the interactions between particles is neglected. Therefore we will approximate the matter accretion as if it were an ideal gas, Furthermore, since the system has to be chemically neutral, the number of positive and negative charges must be equal. In addition, the number of particles from the second and third generations (e.g. muons and tauons) in the matter stream must be ignorable.

We can determine how much of the accreted mass is composed of protons and electrons very simply by compatin the proton mass $m_p 938\ MeV/c^2$ ($1.672\times 10^{-27}\ kg$) and the electron $m_e = 0.511\ MeV/c^2$ ($9.109 \times 10^{-31} kg$), which would imply that the protons contribute $\simeq 99.95$ % of the total accreting mass. Thus, for every 1 kg transferred to the neutron star from the donor, 0.9995 kg will be protons and 0.0005 kg will be electrons. After this, we can simply determine how many of each particle is accreted. In the most general sense, we will represent this fraction as $\frac{m_l}{m_p}$, where m_l is the mass of the lepton and m_p is the mass of the proton.

Calculating Mass Loss Rate

A simple model for the change in particle number can be constructed by assuming the neutron star is electrically neutral. Therefore, there must always be, at any given moment, equal numbers of negatively and positively

charged particles. Furthermore, we already assumed that $\mu_e + \mu_p = 0$. Since the accretion disc itself is donating particles to the neutron star, the chemical potential for each particle species in the neutron star must necessarily increase while maintaining chemical equilibrium.

We can obtain a time dependent relation for the mass which will in turn allow us to determine the change in particle number δN_t at time t. Assume that individual particles from the donor star are in free-fall towards the accreting star. By conservation of energy

$$\frac{1}{2} m_l {v_{ff}}^2 = \frac{G M_* m_l}{R} \tag{5.4}$$

where m_l is the mass of particle species l, v_{ff} is the free-fall velocity of the relevant particle, M_* is the mass of the neutron star, and R is the distance between the center of mass of the neutron star and the particle itself.

The luminosity $\mathcal{L}$ is defined as the change in energy as a function of time, which is

$$\mathcal{L} = \frac{1}{2} \frac{dm_l}{dt} {v^2}_{ff} \tag{5.5}$$

It should be noted that not all of the matter being lost from the donor star is actually accreted onto the primary, as some of it is released as heat. The *accretion efficiency* η is defined as

$$\eta = \frac{G M_* m_l}{R c^2} \tag{5.6}$$

From Eq 5.4, the free-fall velocity is easily determined

$$v_{ff} = \sqrt{\frac{2GM_*}{R}} \tag{5.7}$$

plugging 5.7 into 5.5, we obtain the luminosity as

$$\mathcal{L} = \frac{1}{2}\frac{dM}{dt}v^2{}_{ff} = \frac{1}{2}\frac{c^2}{c^2}\frac{2GM_*}{R}\frac{dM}{dt} = \eta\dot{M}c^2 \tag{5.8}$$

For a neutron star of mass $M_* \approx 1M_{Sun}$ and radius $R \approx 10km$, the efficiency $\eta \approx .1$

When the accreting binary system is in hydrodynamic equilibrium, it is accreting at its maximum rate. This also entails that the luminosity is at the maximum as well. In this state, we can define the *Eddington accretion rate* $\dot{M}_{Edd}$ and the *Eddington luminosity* $\mathcal{L}_{Edd}$. The Eddington luminosity can be obtained by considering the spherically accreting case, although this is also a good approximation for the disc accretion as well [**?**]

Let $F_{grav} = F_{rad}$, where F_{grav} is the gravitational force acting on a single particle and F_{rad} is the force of the radiation pressure coming from the photons that are generated as they strike the surface of the neutron star. From Newton's law of gravitation,

$$F_{grav} = \frac{GM_*(m_p + m_e)}{R^2} \approx \frac{GM_*m_p}{R^2} \tag{5.9}$$

since $m_p/m_e \approx 1876$. F_{rad} can be related to the $Thomson\ cross-section\ \sigma_T$, which can be defined as

$$\sigma_T = \frac{8\pi}{3}\left(\frac{\alpha\lambda_e}{2\pi}\right)^2 \tag{5.10}$$

where α is the fine structure constant $\approx 1/137$ and $\lambda_e = \frac{h}{m_e c}$ is the Compton wavelength for the electron. Therefore,

$$F_{rad} = p\Phi\sigma_T \tag{5.11}$$

where Φ, known as $flux$ is the number of photons passing per unit area per second and p is the momentum per photon. The energy per photon $E = \hbar\omega$, so the flux Φ is

$$\Phi = \frac{\mathcal{L}}{\hbar\omega 4\pi R^2} \tag{5.12}$$

From here, the number of collisions per second can be calculated as

$$number\ of\ collisions = \frac{\mathcal{L}}{\hbar\omega 4\pi R^2}\sigma_T \tag{5.13}$$

$$F_{rad} = \frac{\mathcal{L}\sigma_{\mathcal{T}}}{\hbar\omega 4\pi R^2}\frac{\hbar\omega}{c} = \frac{\mathcal{L}\sigma_T}{4\pi R^2 c} \tag{5.14}$$

Setting Equations 5.9 and 5.14 equal to each other,

$$\frac{GM_* m_p}{R^2} = \frac{\mathcal{L}\sigma_T}{4\pi R^2 c} \tag{5.15}$$

We obtain the following expression for the Eddington luminosity $\mathcal{L}_{Edd}$

$$\mathcal{L}_{Edd} = \frac{4\pi G M_* c m_p}{\sigma_T} \tag{5.16}$$

Notice here that the $\mathcal{L}_{Edd}$ is independent of the temperature and is only dependent upon the mass of the particles and the Thomson cross section. If we equate the luminosities and solve for the mass loss rate at Eddington luminosity,$\dot{M}_{Edd}$, comes out to be

$$\eta\dot{M}_{Edd}c^2 = \frac{4\pi G M_* c m_p}{\sigma_T} \tag{5.17}$$

Therefore,

$$\dot{M}_{Edd} = \frac{4\pi G M_* m_p}{\eta c \sigma_T} \tag{5.18}$$

Notice here that with the exception of M_* on the right side, all the other terms are constant. Therefore, we will define a constant ζ such that

$$\zeta \equiv \frac{4\pi G m_p}{c\sigma_T} \tag{5.19}$$

Thus, we now have an equation that turns in separable integral, relating the mass loss rate $\dot{M}$ to the initial mass of the neutron star M_*

$$\dot{M}_{Edd} = \frac{\zeta}{\eta} M_* \tag{5.20}$$

$$\delta M_t = M_0 e^{\frac{\zeta}{\eta}(t-t_0)} \tag{5.21}$$

where M_* is the initial mass of the neutron star and t_0 is the initial time from the onset of accretion. Thus, we have the accretion rate in terms of the time parameter t.

Going back to our example of the accreting neutron star, from *LIGO* gravitational wave data of $GW17817$ [20],the maximum mass of a neutron star is constrained to $\approx 2.73\ M_{Sun}$ [20] [31]. Given that constraint, we can determine how long it will take to reach a maximum mass M_{max} from an initial neutron star mass M_*. the neutron star will accrete $1.73 M_{Sun}$ to reach M_{max}. If the Thomson cross section is $6.6524 \times 10^{-29}\ m^2$,and the efficiency $\eta = .1$, then $\zeta = 7.02 \times 10^{-16}\ s^{-1}$ If we assume an initial mass of $1 M_{Sun} = 1.989 \times 10^{30}\ kg$ and we let $t_0 = 0$ and we consider the time period of 1 year ($t_f = 3.154 \times 10^7\ s$)

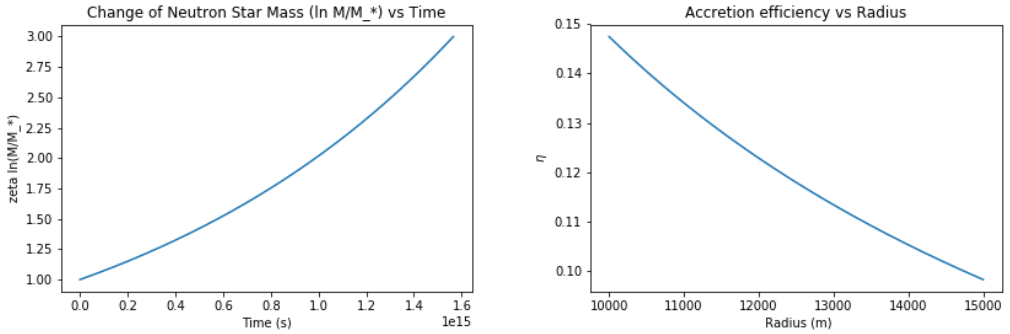

(a) (b)

Figure 5.1: (a) For steady state accreting systems, the rate of accretion is rapid as $\ln(M/M_*)$ changes. In (b) efficiency drops off as radius increases

$$\delta M_t = M_{Sun}\ (7.02 \times 10^{-16}\ s^{-1})(3.154 \times 10^7\ s) = 2.2 \times 10^{-8} M_{Sun} \tag{5.22}$$

Figure 5.1a shows the change in mass fraction as a function of time with (M/M*) on a logarithmic axis. This would indicate a gentle increase early on in the accretion process and a more rapid accretion beginning at $\sim 5^{14}$ years. In Figure 5.1b, we observe a decrease in efficiency as the radius increases. Therefore, we can infer that neutron stars with larger radii will dissipate heat more slowly than those with larger radii. Effectively, this means larger stars, given the definition of efficiency η given earlier, can accrete mass more effectively than smaller stars.

Given that M_t is the total mass being transferred, and it was stipulated earlier that we are only concerned with the electron component of the accretion flow, the total electronic mass M_{e^-} accreting onto the neutron star in time is

$$M_{e^-} = \frac{m_l}{m_p} M_* e^{\frac{\zeta}{\eta}(t-t_0)} \tag{5.23}$$

To obtain the final expression for $N_l(N_{e0}, t)$ explicitly, we must first divide M_t by the reduced electron-proton mass $\mu_{ep} = \frac{m_p m_e}{m_p + m_e}$ and setting it equal to $\delta N(t)$. The reduced mass μ_{ep} is used instead of the electron mass m_e when we consider that, while the electrons are not bound to the protons in ionized hydrogen, for the matter stream for the donor to remain electrically neutral, a kind of *pairing* must be present in such a way that the lighter electron *drags* the heavier proton with it.

Furthermore, we must consider that most of the electrons and protons will participate in weak interactions to form more neutrons. Therefore, we define a dimensionless parameter $\Gamma << 1$ that represents the fraction of electrons that remain free once they are accreted. Thus, our final expression is

Thus

$$N_l(N_{e0}, t) = \frac{4\pi\mu_l^3}{{m_l}^3}\left[\frac{1}{3\beta^3{m_l}^3} - \frac{eB}{\beta{m_l}^3}\left(\frac{m^2}{\mu_l^2}\right)\left(1 - \frac{m}{\mu_l}\right)\right] + \Gamma\frac{m_l}{m_p\mu_{ep}}M_* e^{\frac{\zeta}{\eta}(t-t_0)} \tag{5.24}$$

From this expression, the chemical composition of different lepton species can be obtained with the corresponding background [8] [23]. The determination of the chemical composition also indicates the size of the neutron star given a particular model. [8] [35]

Limitations on the Accretion Rate

We must also note here that in a viscous disc, particles will rub against each other, causing them to radiate. The radiation pressure acts on the accreting matter with a tendency to push the particles away from the neutron star. As long as $F_{rad} = F_{grav}$, hydrodynamic equilibrium will be maintained and

accretion will continue. However, if $F_{rad} > F_{grav}$, the neutron star, in principle, will not accrete, and the system itself is in no longer in hydrodynamic equilibrium. Additionally, the effective surface temperature and luminosity of the star increases, so $\mathcal{L}_{edd}$ sets an upper limit to how fast mass will accrete to the neutron star in hydrodynamic equilibrium. [32]. If $F_{rad} < F_{grav}$, then the system becomes unstable, leading to complete gravitational collapse of the system.

As such, we can determine a criterion under which accretion will occur, and when the binary system is not sufficiently luminous enough to resist gravitational collapse. When $F_{rad} > F_{grav}$,

$$\mathcal{L} > \frac{4\pi G M_* c m_p}{\sigma_T} \tag{5.25}$$

Approximating the neutron star as a blackbody, then the luminosity $\mathcal{L}$ can also be expressed as

$$\mathcal{L} = \sigma_{SB} A T^4 \tag{5.26}$$

where $\sigma_{SB} = 5.67 \times 10^{-8} W \cdot m^{-2} \dot{K}^{-4}$ is the $Stefan-Boltzmann\ constant$, A is the surface area of the neutron star, and T is the effective temperature. Replacing $\mathcal{L}$ in 5.25 with 5.26, and rearranging,

$$T_c > \sqrt[4]{\frac{4\pi G M_* c m_p}{\sigma_{SB} A \sigma_T}} \approx 10^6 K = 86\ eV \tag{5.27}$$

Thus, we obtain a critical temperature T_c which, if greatly exceeded, will cut off the accretion process for a star $M_* = M_{Sun}$. If the temperature is much less than this, the neutron star is not hot enough to maintain hydrodynamic equilibrium, and will therefore collapse.

Discussion

In summary, the particle number density for the e^- (assuming the e^+ contribution is negligible) for a neutron star in a magnetic field B was obtained using a straightforward Fermi-Dirac distribution. A time-dependent expression for the particle number density $N(t) = \frac{4\pi\mu_l^3}{{m_l}^3}\left[\frac{1}{3\beta^3{m_l}^3} - \frac{eB}{\beta{m_l}^3}\left(\frac{{m_l}^2}{\mu_l^2}\right)\left(1 - \frac{m_l}{\mu_l}\right)\right] + \Gamma\frac{m_l}{m_p\mu_{ep}}M_* e^{\frac{\zeta}{\eta}(t-t_0)}$ was obtained for an accreting neutron star binary system for a 'high' efficiency system with $\eta = .1$, and by extension, we can determine the chemical composition of an accreting neutron star of initial mass M_* at time t. The efficiency would account for radiation pressure that would inhibit the accretion efficiency In Figure 5.1a, we showed that, assuming a steady state disc with negligible viscosity, this shows a gentle accretion of matter for the duration of $\simeq 10^{15}\ s\ (\simeq 10^7\ years)$, which is consistent for a young LMXB. For the lifetime of a HMXB, it is suitable to adjust parameters ζ or η to be consistent with the observed lifetime. For an accreting neutron star, an upper limit to the accretion rate is determined when the critical temperature $T_c \simeq 86eV \simeq 10^6 K$

It is desirable to know what factors tend to most affect the number density of charged particles. In Figures 5.2a and 5.2b, we plot the change in number density as a function of both the magnetic field and the chemical potential. These 3D graphs indicate the change in the number density of electron with the increasing chemical potential and the magnetic field. The magnetic field in Gauss is plotted on a semi-logarithmic scale with a range of $10^8 - 10^{13}\ G$ on one axis and the chemical potential ranging from $70 - 200\ MeV$ plotted on the other axis in the same plane. These ranges of chemical potential and

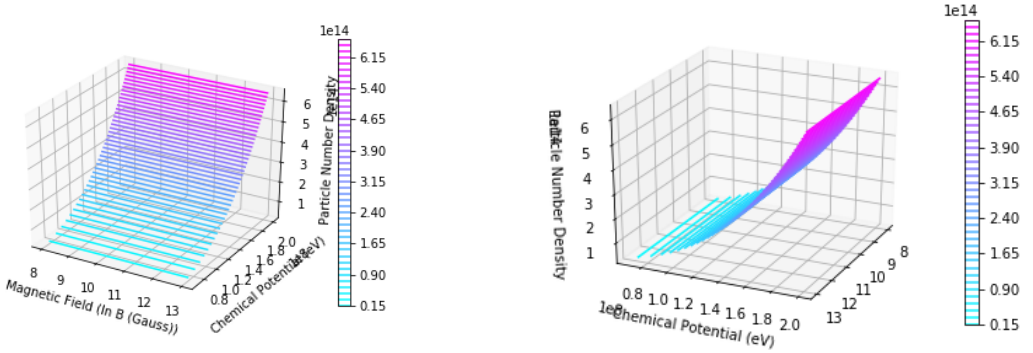

(a) (b)

Figure 5.2: Contour plots featuring showing the change in number density as a function of chemical potential and magnetic field. The right figure is a rotation of the left

the magnetic field are relevant for neutron stars. On the vertical axis is the change in number density as a function of both the magnetic field and the chemical potential. It is apparent that the chemical potential affects the

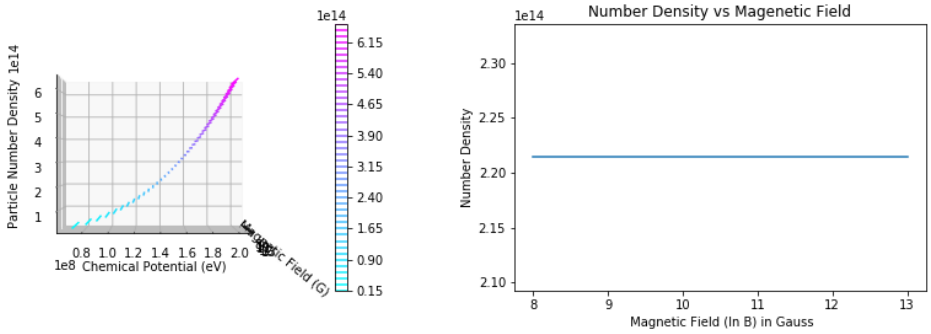

(a) (b)

Figure 5.3: In (a), The particle number density increases with chemical potential. On the other hand, in (b),particle number density remains constant with increasing magnetic field

number density to a much greater degree than the magnetic field strength. To illustrate this further, Figures 5.3a and 5.3b are a cross section of the

contour plot which effectively show the number density vs magnetic field and number density vs. chemical potential, respectively. When number density vs chemical potential is examined, the number density ranges from $\sim 10^{13} - 10^{14}$, starting off gradually for $70 \leq \mu_l \leq 100\ MeV$ and rapidly increasing afterwards. However, if we look at the number density vs. magnetic field plot, we don't see very much change at all, if any, throughout the entire range of magnetic field strengths, which is expected. It is expected that the magnetic field will affect the orientation of the charged particles in the neutron star region. Therefore, we determine that the chemical potential is the most relevant quantity to determine the particle number density of charged particles, as expected.

Future Work

To take this project further, the next step would be to derive an expression for the dynamical magnetization for the electrons. $\mathcal{M}_\uparrow(t)$. When that is accomplished, it would then be straightforward to obtain an expression for the dynamic potential $\Omega_e(t)$. Additionally, different fluid models for the accretion may be tested including viscous models, superfluid models, and relativistic plasmas (QED and QCD plasmas). Finally, we would like to see how the critical density ρ_c (the density at which black holes form) and the critical number density N_c (the density at which quantum magnetic collapse occurs) coincides, if at all. If not, this may present some interesting scenarios where we have an instability due to the anistotropic pressures before the critical density ρ_c is reached.

BIBLIOGRAPHY

[1] Pandharipande, V. R., Ravenhall, D. G., & Akmal, A. (1998). Many body theory of nuclear and neutron star matter. To Appear in the 26th International Workshop on Gross Proper, pp. 11–28. Retrieved from http://inspirehep.net/record/467215

[2] Baade, W., & Zwicky, F. (1934). On super-novae. *Proceedings of the National Academy of Sciences of the United States of America*, 20(5), 254–259. https://doi.org/10.1073/PNAS.20.5.254

[3] Baym, G., & Pethick, C. (1979). Physics of neutron stars. *Annual Review of Astronomy and Astrophysics, 17(1), 415–443.* https://doi.org/10.1146/annurev.aa.17.090179.002215

[4] Hewish, A., Bell, S. J., Pilkington, J. D. H., Scott, P. F., & Collins, R. A. (1968). Observation of a rapidly pulsating radio rource. *Nature*, 217(5130), 709–713. https://doi.org/10.1038/217709a0

[5] Benacquista, M. J.,& Downing, J. M. B. (2013). Relativistic binaries in globular clusters. *Living Reviews in Relativity*, 16(1), 4. http://doi.org/10.12942/lrr-2013-4

[6] Bonanno, A., & Urpin, V. (2015). *The accretion rate and minimum spin period of accreting pulsars. Monthly Notices of the Royal Astronomical Society. http://doi.org/10.1093/mnras/stv1112*

[7] Carroll, B. W., & Ostlie, D. A. *An introduction to modern astrophysics.* San Francisco, CA: Pearson/Addison Wesley, 2009.

[8] Chaichian, M., Masood, S. S., Montonen, C., Martinez, A. P., & Rojas, H. P. (1999). Quantum magnetic collapse. http://doi.org/10.1103/PhysRevLett.84.5261

[9] Chandra X-ray Observatory

[10] Degenaar, N., Pinto, C., Miller, J., Wijnands, R., Altamirano, D., Paerels, F., ... Chakrabarty, D. (2018). An in-depth study of a neutron star accreting at low Eddington rate: On the possibility of a truncated disc and an outflow. *Mon. Not. R. Astron. Soc*, 000. Retrieved from https://www.sron.nl/spex

[11] Fermi Gamma-ray Space Telescope

[12] Giacconi, R., Gursky, H., Paolini, F. R., & Rossi, B. B. (1962). Evidence for x-rays from sources outside the solar system. *Physical Review Letters*, 9(11), 439–443. https://doi.org/10.1103/PhysRevLett.9.439

[13] Gold, T. (1968). rotating neutron stars as the origin of the pulsating radio sources. *Nature*, 218(5143), 731–732. https://doi.org/10.1038/218731a0

[14] Hansson, J., & Sandin, F. (2004). *Preon stars: a new class of cosmic compact objects*. https://doi.org/10.1016/j.physletb.2005.04.034

[15] Kaspi, V. M., & Beloborodov, A. (2017). Magnetars. https://doi.org/10.1146/annurev-astro-081915-023329

[16] Konar, S. (2013). Evolution of the magnetic field in accreting neutron stars. Retrieved from http://arxiv.org/abs/1308.2184

[17] Lamb, F. K., & Boutloukos, S. (2007). Accreting neutron stars in low-mass x-ray binary systems. Retrieved from https://arxiv.org/pdf/0705.0155.pdf

[18] Landau, L. D., & Lifshitz, E. M. (2010). The classical theory of fields. Oxford: Butterworth Heinemann

[19] Liu, Q. Z., Van Paradijs, J., & Van Den Heuvel, E. P. J. (2007). A catalogue of low-mass X-ray binaries in the Galaxy, LMC, and SMC (Fourth edition). Retrieved from http://isdc.unige.ch/

[20] Margalit, B., & Metzger, B. (2017). Constraining the maximum mass of neutron stars From multi-messenger observations of GW170817. https://doi.org/10.3847/2041-8213/aa991c

[21] Melia, F. (2009). *High-energy astrophysics*. Princeton: Princeton University Press.

[22] Martinez, A. P., Rojas, H. P., & Cuesta, H. J. M. (2003). Magnetic collapse of a neutron gas: Can magnetars indeed be formed. https://doi.org/10.1140/epjc/s2003-01192-6

[23] Masood, S. S. (1993). Neutrino physics in hot and dense media. *Physical Review D*, 48(7), 3250–3258. https://doi.org/10.1103/PhysRevD.48.3250

[24] Masood, Samina. (1993). Renormalization of QED in superdense media. *Physical review D: Particles and fields*. 47. 648-652. 10.1103/PhysRevD.47.648. and references therein.

[25] Negueruela, I., Smith, D. M., Reig, P., Chaty, S., & Torrejón, J. M. (2005). *Supergiant fast x-ray transients: A new class of high mass x-ray binaries unveiled by INTEGRAL.* Retrieved from https://arxiv.org/pdf/astro-ph/0511088.pdf

[26] Ögelman, H. 1995 in Lives of Neutron Stars, ed. M.A. Alpar, . Kiziloglu and J. van Paradijs, (Kluwer, Dordrecht)

[27] Olausen, S. A., & Kaspi, V. M. (2013). *The McGill magnetar catalog.* https://doi.org/10.1088/0067-0049/212/1/6

[28] Oppenheimer, J. R., & Volkoff, G. M. (1939). On massive neutron cores. *Physical Review*, 55(4), 374–381. https://doi.org/10.1103/PhysRev.55.374

[29] Özel, F. (2012). Surface emission from neutron stars and implications for the physics of their interiors. Retrieved from https://arxiv.org/pdf/1210.0916.pdf

[30] Ozel, F., Baym, G., & Guver, T. (2010). Astrophysical measurement of the equation of state of neutron star matter. https://doi.org/10.1103/PhysRevD.82.101301

[31] Pankow, C. (2018). On GW170817 and the galactic binary neutron star population. https://doi.org/10.3847/1538-4357/aadc66

[32] Pringle, E., J., Rees, & J., M. (1972, October 01). Accretion disc models for compact x-ray sources. *Astron-*

omy and Astrophysics, Vol. 21, p. 1 (1972). Retrieved from http://adsabs.harvard.edu/abs/1972A&A....21....1P

[33] Rojas, H. P., & Querts, E. R. (2006). Vacuum pressures in a strong magnetic field and casimir forces. *The Tenth Marcel Grossmann Meeting. doi* : $10.1142/9789812704030_0308$

[34] Rosswog, S., & Brügen, M. *Introduction to high-energy astrophysics.* Cambridge: Cambridge Univ. Press, 2010.

[35] Shapiro, S. L., Teukolsky, S. A., & Lightman, A. P. (1983). *Black Holes, White Dwarfs, and Neutron Stars: The Physics of Compact Objects.* Physics Today. http://doi.org/10.1063/1.2915325

[36] Schmidt, M., & M. (1963). 3C 273 : A star-like object with Large redshift. *Nature*, 197(4872), 1040–1040. https://doi.org/10.1038/1971040a0

[37] Shakura, N. I., & Sunyaev, R. A. (1973). Black holes in binary systems: Observational appearances. *Symposium - International Astronomical Union*, 55, 155-164. doi:10.1017/s007418090010035x

[38] Steiner, A. W., Lattimer, J. M., & Brown, E. F. (2010). The equation of state from observed masses and radii of neutron stars. *The Astrophysical Journal*, 722(1), 33–54. https://doi.org/10.1088/0004-637X/722/1/33

[39] Strohmayer, T., & Bildsten, L. (2006). New views of thermonuclear bursts. In W. Lewin & M. Van der Klis (Eds.), *Compact Stellar X-ray Sources* (Cambridge Astrophysics, pp. 113-156). Cambridge: Cambridge University Press. doi:10.1017/CBO9780511536281.004

[40] Neil Gehrels Swift Observatory

[41] Tauris, T. M., & Heuvel, E. van den. (2003). Formation and evolution of compact stellar x-ray sources. Retrieved from http://arxiv.org/abs/astro-ph/0303456

[42] Thompson, M. J. (2006). *An introduction to astrophysical fluid dynamics*. London: Imperial College Press.

[43] Watts, A. L., Andersson, N., Chakrabarty, D., Feroci, M., Hebeler, K., Israel, G., ... van der Klis, M. (2016). Measuring the neutron star equation of state using X-ray timing. http://doi.org/10.1103/RevModPhys.88.021001

[44] Woods, P., & Thompson, C. (2006). Soft gamma repeaters and anomalous X-ray pulsars: Magnetar candidates. In W. Lewin & M. Van der Klis (Eds.), *Compact Stellar X-ray Sources* (Cambridge Astrophysics, pp. 547-586). Cambridge: Cambridge University Press. doi:10.1017/CBO9780511536281.015

[45] Yakovlev, D. G., & Pethick, C. J. (2004). Neutron star cooling. *Annual Review of Astronomy &Astrophysics*, Vol. 42, Issue 1, Pp.169-210, 42, 169–210. https://doi.org/10.1146/annurev.astro.42.053102.134013

[46] Zhang, N.-B., Li, B.-A., & Xu, J. (2018). Combined constraints on the equation of state of dense neutron-rich matter from terrestrial txperiments and observations of neutron stars. https://doi.org/10.3847/1538-4357/aac027